Genomic investigation of the strawberry pathogen *Phytophthora fragariae* indicates pathogenicity is determined by transcriptional variation in three key races

Thomas M. Adams[1,2¤], Andrew D. Armitage[1], Maria K. Sobczyk[1†], Helen J. Bates[1], Javier F. Tabima[3], Brent A. Kronmiller[4], Brett M. Tyler[3,4], Niklaus J. Grünwald[5], Jim M. Dunwell[2], Charlotte F. Nellist[1*] and Richard J. Harrison[1,6]

[1]Department of Genetics, Genomics and Breeding, NIAB EMR, New Road, East Malling, Kent, ME19 6BJ, UK.

[2]School of Agriculture, Policy and Development, University of Reading, Reading, Berkshire, RG6 6AH, UK.

[3]Department of Botany and Plant Pathology, Center for Genome Biology and Biocomputing, Oregon State University, Corvallis, OR, USA.

[4]Center for Genome Biology and Biocomputing, Oregon State University, Corvallis, OR, 97331, USA.

[5]Horticultural Crops Research Unit, Agricultural Research Service, United States Department of Agriculture, Corvallis, OR, USA.

[6] NIAB Cambridge Crop Research, NIAB, Huntingdon Road, Cambridge, CB3 0LE, UK.

¤ Current address: Department of Crop Genetics, John Innes Centre, Norwich Research Park, Norwich, NR4 7UH, UK.

† Current address: University of Bristol, Oakfield House, Oakfield Grove, Clifton, BS8 2BN, UK.

***Correspondence:**

Charlotte F. Nellist

charlotte.nellist@emr.ac.uk

ABSTRACT

The oomycete *Phytophthora fragariae* is a highly destructive pathogen of cultivated strawberry (*Fragaria* × *ananassa*), causing the root rotting disease, 'red core'. The host-pathogen interaction has a well described gene-for-gene resistance relationship, but to date neither candidate avirulence nor resistance genes have been identified. We sequenced a set of American, Canadian and UK isolates of known race type, along with three representatives of the closely related pathogen of the raspberry (*Rubus idaeus*), *Phytophthora rubi*, and found a clear population structure, with a high degree of nucleotide divergence seen between some race types and abundant private variation associated with race types 4 and 5. In contrast, between isolates defined as UK races 1, 2 & 3 (UK1-2-3) there was no evidence of gene loss or gain; or the presence of insertions/deletions (INDELs) or Single Nucleotide Polymorphisms (SNPs) within or in proximity to putative pathogenicity genes could be found associated with race variation. Transcriptomic analysis of representative UK1-2-3 isolates revealed abundant expression variation in key effector family genes associated with pathogen race; however, further long read sequencing did not reveal any long range polymorphisms to be associated with avirulence to race UK2 or UK3 resistance, suggesting either control in *trans* or other stable forms of epigenetic modification modulating gene expression. This work reveals the combined power of population resequencing to uncover race structure in pathosystems and *in planta* transcriptomic analysis to identify candidate avirulence genes. This work has implications for the identification of putative avirulence genes in the absence of associated expression data and points towards the need for detailed molecular characterisation of mechanisms of effector regulation and silencing in oomycete plant pathogens.

INTRODUCTION

Phytophthora fragariae, the causal agent of red core or red stele root rot, is a highly destructive pathogen of cultivated strawberry (*Fragaria* × *ananassa*), resulting in whole plant collapse. The majority of commercial strawberries grown in the UK are grown on table tops using soilless substrate, under polytunnels or in glasshouses (Robinson Boyer et al., 2016). *Phytophthora* spp. are a particular problem in these systems due to the ease of spread through the irrigation system via the motile zoospores. Since the first report in Scotland in 1920, this disease has spread to the majority of strawberry growing regions, except China and the Southern Mediterranean regions of Europe (van de Weg, 1997b; EFSA Panel on Plant Health (PLH), 2014). Currently, it is treated as a quarantine pest by the European and Mediterranean Plant Protection Organization (EPPO), where it is listed as an A2

60 pest (van de Weg, 1997b; EPPO, 2018). The classification of this pathogen has proven controversial,
61 as initially the organism was identified as a single species (Hickman, 1941), but when a *Phytophthora*
62 disease of raspberry (*Rubus idaeus*) was discovered, it was reclassified as *P. fragariae* var. *fragariae*
63 (Wilcox et al., 1993). More recently, the pathogens have been separated into distinct species, *P.*
64 *fragariae* and *Phytophthora rubi*, affecting strawberry and raspberry respectively. This was supported
65 by sequence analysis of key loci (Man in 't Veld, 2007), as well as whole genome analyses (Tabima
66 et al., 2018).

67 It has previously been proposed that the ability of different isolates of *P. fragariae* to cause
68 disease on a variety of *F.* × *ananassa* cultivars can be explained by a gene-for-gene model (van de
69 Weg, 1997a). The model is currently thought to consist of at least eleven resistance genes in *F.* ×
70 *ananassa* with eleven corresponding avirulence factors in *P. fragariae* (W. E. van de Weg,
71 Wageningen University and Research, The Netherlands, personal communication). The development
72 of race schemes is country dependent and ones exist for the UK, USA and Canada.

73 All publicly available genome assemblies of *P. fragariae* have to date solely utilised Illumina
74 short read sequencing technologies, resulting in assemblies of 73.68 Mb and 76 Mb, in 1,616 and
75 8,511 scaffolds respectively (Gao et al., 2015; Tabima et al., 2017). Recently, long read sequencing
76 technology has been shown to provide assemblies of improved contiguity for *Phytophthora*
77 pathogens, specifically the generation of the haplotype-phased assembly of *Phytophthora ramorum*
78 (60.5 Mb in 302 primary contigs) using PacBio sequencing (Malar et al., 2019) and the assembly of
79 *Phytophthora capsici* (95.2 Mb in 424 scaffolds) using Oxford Nanopore Technology (Cui et al.,
80 2019).

81 Pathogenomic investigations in *Phytophthora* species of pathosystems with similar gene-for-
82 gene models of resistance have shown a variety of mechanisms through which variation in virulence
83 can be controlled. For instance, in *Phytophthora sojae*, the *Avr1d* gene was identified as an RxLR
84 effector recognised by the *Rps1d* resistance gene in soybean (Yin et al., 2013). Studies of the RxLR
85 effector *PiAvr4* from *Phytophthora infestans* showed that it was always present in isolates avirulent
86 on potato plants containing the resistance gene *R4*, whereas virulent isolates possessed a frameshift
87 mutation producing a truncated protein (van Poppel et al., 2008). In comparison, *Avr3c* in *P. sojae*
88 was identified in both virulent and avirulent isolates on soybean plants containing *Rps3c*, but in
89 virulent isolates the gene displayed several polymorphisms resulting in a change to the amino acid
90 sequence leading to a failure of recognition by the plant (Dong et al., 2009). Recently, investigations
91 of the EC-1 clonal lineage of *P. infestans* revealed a variation of the ability of isolates to cause disease

92 on potato plants possessing the *Rpi-vnt1.1* gene. It was shown, in the absence of genetic mutations,
93 that differences in the expression level of *Avrvnt1* were detected and these correlated with virulence
94 (Pais et al., 2018).

95 In this study, we assembled and annotated a population of isolates of *P. fragariae* and the
96 related pathogen of raspberry, *P. rubi*. We identified a subpopulation of *P. fragariae* isolates
97 representing three distinct pathogenicity races (UK1-2-3). This subpopulation was found to be
98 remarkably similar in gene complement, as well as showing little divergence at the nucleotide
99 sequence level. To further investigate the cause of the observed variation in pathogenicity phenotypes,
100 transcriptomic datasets were generated for representative isolates of each pathogenicity race in this
101 subpopulation. This revealed expression level polymorphisms between the isolates, allowing for the
102 generation of candidate lists for *PfAvr1*, *PfAvr2* and *PfAvr3*. A strong candidate for *PfAvr2*,
103 PF003_g27513 was identified as expressed in the BC-16 and A4 (UK2) isolates, yet not expressed in
104 the BC-1 (UK1) and NOV-9 (UK3) isolates. A candidate for *PfAvr3* was also identified,
105 PF009_g26276; it is expressed in NOV-9 (UK3), yet not expressed in BC-1 (UK1), A4 (UK2) and
106 BC-16 (UK2) isolates. Additional sequencing did not reveal long-range polymorphisms influencing
107 the expression of these candidate genes; we therefore suggest control may be in *trans* or due to
108 epigenetic factors.
109

110 # MATERIALS AND METHODS

111 ## Isolate selection and sources

112 A selection of ten isolates of *P. fragariae* were sourced from the Atlantic Food and Horticulture
113 Research Centre (AFHRC), Nova Scotia, Canada. An additional isolate of *P. fragariae*, SCRP245,
114 alongside three *P. rubi* isolates, were sourced from the James Hutton Institute (JHI), Dundee, Scotland
115 (detailed in **Table 1**).

116 ## Culturing of isolates

117 All work with *P. fragariae* and *P. rubi* was conducted in a Tri-MAT Class-II microbiological safety
118 cabinet. Isolates were routinely subcultured on kidney bean agar (KBA) produced as previously
119 described (Maas, 1972). Isolates were grown by transferring two pieces of between 1 and 4 mm^2 onto
120 fresh KBA plates, subsequently sealed with Parafilm®. Plates were then grown at 20°C in the dark in
121 a Panasonic MIR-254 cooled incubator for between seven and fourteen days.

122 Mycelia were also grown in liquid pea broth, produced as previously described (Campbell et
123 al., 1989) with the addition of 10 g/L sucrose. These plates were inoculated with five pieces (1 - 4
124 mm^2) of mycelium and media, subsequently sealed with Parafilm®. These were grown at 20 °C for
125 four to five days in constant darkness.

126 Pathogenicity testing of isolates

127 Mother stock plants of *F.* × *ananassa* were maintained in 1 L pots in polytunnels. Runner plants were
128 pinned down into 9 cm diameter pots filled with autoclaved 1:1 peat-based compost:sand. The clones
129 were grown on for three weeks to establish their own root system and then were cut from the mother
130 plant. Inoculations were performed as described previously (van de Weg et al., 1996). Plants were
131 placed in a growth chamber with 16/8 hour light/dark cycle at a constant 15 °C. Inoculated plants
132 stood in a shallow layer of tap water (2 - 7 mm) for the entire experiment and were watered from
133 above twice a week. After six weeks, plants were dug up and the roots were rinsed to remove the
134 soil/sand mix. Roots were then assessed for distinctive disease symptoms of 'rat's tails', which is the
135 dieback from the root tip and 'red core', which is the red discolouration of the internal root visible
136 when longitudinally sliced open. Samples for which infection was unclear were visualised under a
137 light microscope for the presence of oospores. This was performed through squash-mounting of the
138 root tissue, where a sample of root was excised and pressed between a microscope slide and cover
139 slip. This sample was then examined at 40x magnification under high light intensity with a Leitz
140 Dialux 20 light microscope.

141 Sequencing of DNA

142 For Illumina sequencing, gDNA was extracted from 300 mg of freeze-dried mycelium using the
143 Macherey-Nagel NucleoSpin® Plant II Kit. The manufacturer's protocol was modified by doubling
144 the amount of lysis buffer PL1 used, increasing the incubation following RNase A addition by five
145 minutes, doubling the volume of buffer PC and eluting in two steps with 35 µL of buffer PE warmed
146 to 70 °C. For PacBio and Oxford Nanopore Technologies (ONT) sequencing, gDNA was extracted
147 using the Genomic-Tip DNA 100/G extraction kit, following the Tissue Sample method.
148 To create Illumina PCR-free libraries, DNA was sonicated using a Covaris M220 and size-
149 selected using a BluePippin BDF1510 1.5% gel selecting for 550 bp. Libraries were constructed using
150 the NEBNext enzymes: End repair module (E6050), A-TAiling module (E6053), Blunt T/A ligase
151 (M0367) and Illumina single-indexed adapters. Sequencing was performed to generate 2 x 300 bp

152 reads on a MiSeq™ system using MiSeq Reagent Kit V3 600 cycle (MS-102-3003). PacBio library
153 preparation and sequencing was performed by the Earlham Institute, UK on a PacBio RS II machine.
154 ONT sequencing libraries were created using the SQK-LSK108 kit following the manufacturer's
155 protocol and sequenced using the FAH69834 FLO-MIN106 flow cell on a GridION for approximately
156 28 hours.

157 **Inoculation time course experiment**

158 Growth of isolates for inoculations were performed on fresh KBA plates for approximately 14 days
159 as described above, before the mycelium had reached the plate edge. Plugs of mycelium growing on
160 agar were taken using a flame sterilised 10 mm diameter cork borer and plugs were submerged in
161 chilled stream water. Plates were incubated in constant light for three days at 13 °C, with the water
162 changed every 24 hours. For the final 24 hours, chilled Petri's solution (Judelson et al., 1993) was
163 used. Roots of micropropagated *F.* × *ananassa* 'Hapil' plants (GenTech, Dundee, UK), maintained
164 on *Arabidopsis thaliana* salts (ATS) media (Taylor et al., 2016), were submerged for one hour before
165 transfering back to ATS plates. These plates were kept at 15 °C, with 16/8 hour light/dark cycle, with
166 a photosynthetic photon flux (PPF) of 150 µmol m^{-2} s^{-1} provided by fluorescent lamps
167 (FL40SSENW37), in a Panasonic MLR-325H controlled environment chamber. Root tissue was
168 harvested at a selection of time points post inoculation by rinsing root tissue successively in three
169 beakers of sterile dH_2O to remove all media. Roots were separated below the crown tissue, flash frozen
170 in liquid nitrogen and stored at -80 °C.

171 Extraction of total RNA from inoculated root tissue was performed similarly to the previously
172 described 3% $CTAB_3$ method (Yu et al., 2012). Briefly, plant material was disrupted under liquid
173 nitrogen in a mortar and pestle, previously decontaminated through cleaning with RNaseZap™
174 solution and baking for 2 hours at 230 °C to deactivate RNAse enzymes. This material was transferred
175 to a warmed extraction buffer (Yu et al., 2012) containing β-mercaptoethanol with 0.01 g of PVPP
176 added per 0.1 g of frozen tissue. The remaining steps were performed as previously described (Yu et
177 al., 2012), except that 60 µL DEPC-treated H_2O was used to elute RNA.

178 Mycelium was grown in liquid pea both and dried on a Q100 90 mm filter paper (Fisher
179 Scientific) using a Büchner funnel and a Büchner flask attached to a vacuum pump. Total RNA was
180 then extracted using the QIAGEN RNEasy Plant Mini kit with the RLC buffer. Extraction was carried
181 out following the manufacturer's instructions with an additional spin to remove residual ethanol.

182 RNA was checked for quality using a NanoDrop 1000 spectrophotometer, quantity with a
183 Qubit 2.0 Fluorometer and integrity with a TapeStation 4200 before being prepared for sequencing
184 via Reverse Transcription-Polymerase Chain Reaction (RT-PCR) and sequencing on an Illumina
185 HiSeq™ 4000 by Novogene, Hong Kong, Special Administrative Region, China. Timepoints for
186 sequencing were selected through the detection of β-tubulin transcripts by RT-PCR. Reverse
187 transcription was performed with the SuperScript™ III Reverse Transcriptase kit with an equal
188 amount of RNA used for each sample. The complementary DNA (cDNA) was then analysed by PCR
189 with 200 μM dNTPs, 0.2 μM of each primer (detailed in **Supplementary Table S1**), 2 μL of cDNA
190 template and 2.5 units of Taq DNA polymerase and the buffer supplied in a 20 μL reaction. Reactions
191 were conducted in a Veriti 96-well thermocycler with an initial denaturation step at 95 °C for 30
192 seconds, followed by 35 cycles of a denaturation step at 95 °C for 30 seconds, an annealing
193 temperature of 60 °C for 30 seconds and an extension step of 72 °C for 30 seconds. This was followed
194 by a final extension step of 72 °C for 5 minutes and held at 10 °C. Products were visualised by gel
195 electrophoresis on a 1% w/v agarose gel at 80 V for 90 minutes, stained with GelRed. Following this,
196 three biological replicates of samples taken at: 24 hpi, 48 hpi and 96 hpi for BC-16, 48 hpi for BC-1
197 and 72 hpi for NOV-9 were sequenced (**Supplementary Figure S1**). Additionally, *in vitro* mycelial
198 RNA was sequenced.
199 *P. rubi* RNA-Seq reads were sequenced on a HiSeq™ 2000 system.

200 Genome assembly

201 Prior to assembly, Illumina reads were cleaned and sequencing adaptors were removed with fastq-mcf
202 (Aronesty, 2013). Quality control of PacBio data was performed by the Earlham Institute, Norwich,
203 UK. ONT reads were basecalled with Albacore version 2.2.7 and adaptors were removed with
204 Porechop version 0.2.0 (Wick, 2018) and the trimmed reads were corrected with Canu version 1.4
205 (Koren et al., 2017).
206 Assemblies of isolates sequenced solely with Illumina data were generated with SPAdes
207 version 3.11.0 (Bankevich et al., 2012) with Kmer sizes of 21, 33, 55, 77, 99 and 127. PacBio reads
208 were assembled using FALCON-Unzip (Chin et al., 2016). FALCON version
209 0.7+git.7a6ac0d8e8492c64733a997d72a9359e1275bb57 was used, followed by FALCON-Unzip
210 version 0.4.0 and Quiver (Chin et al., 2013). Error corrected ONT reads were assembled using
211 SMARTdenovo version 1.0.0 (Ruan, 2018).

212 Following assembly, error correction was performed on ONT assemblies by aligning the reads
213 to the assembly with Minimap2 version 2.8r711-dirty (Li, 2018) to inform ten iterations of Racon
214 version 1.3.1 (Vaser et al., 2017). Following this, reads were again mapped to the assembly and errors
215 were corrected with Nanopolish version 0.9.0 (Simpson, 2018). PacBio and ONT assemblies had
216 Illumina reads mapped with Bowtie 2 version 2.2.6 (Langmead and Salzberg, 2012) and SAMtools
217 version 1.5 (Li et al., 2009) to allow for error correction with ten iterations of Pilon version 1.17
218 (Walker et al., 2014).
219 Following assembly, all contigs smaller than 500 bp were discarded and assembly statistics
220 were collected using Quast version 3.0 (Gurevich et al., 2013). BUSCO statistics were collected with
221 BUSCO version 3.0.1 (Simão et al., 2015) using the eukaryota_odb9 database on the assemblies, as
222 the stramenopile database was not available at the time of the analysis. Identification of repetitive
223 sequences was performed with Repeatmasker version open-4.0.5 (Smit et al., 2015) and
224 RepeatModeler version 1.73 (Smit and Hubley, 2015). Transposon related sequences were identified
225 with TransposonPSI release 22nd August 2010 (Haas, 2010).

226 Prediction of gene models and effectors

227 Gene and effector prediction was performed similarly to a previously described method (Armitage et
228 al., 2018). Firstly, raw RNA-Seq reads of BC-16 from both mycelial samples and the inoculation time
229 course were cleaned with fastq-mcf (Aronesty, 2013). Reads from the inoculation time course were
230 first aligned to the *Fragaria vesca* version 1.1 genome (Shulaev et al., 2011) with STAR version
231 2.5.3a (Dobin et al., 2013) and unmapped reads were kept. These unmapped reads and those from *in*
232 *vitro* mycelium were mapped to the assembled *P. fragariae* genomes with STAR (Dobin et al., 2013).
233 RNA-Seq data from *P. rubi* were aligned to *P. rubi* assemblies with the same method. Further steps
234 were performed as previously described (Armitage et al., 2018). Additionally, putative apoplastic
235 effectors were identified through the use of ApoplastP (Sperschneider et al., 2018). Statistical
236 significance of the differences between predicted numbers of effector genes was assessed with a
237 Welch two sample t-test in R version 3.4.3 (R core team, 2017).

238 Gene orthology analysis

239 Orthologue identification was performed using OrthoFinder version 1.1.10 (Emms and Kelly, 2015)
240 on predicted proteins from all sequenced *P. fragariae* and *P. rubi* isolates. Orthogroups were
241 investigated for expanded and unique groups for races UK1, UK2 and UK3. Unique orthogroups were

242 those containing proteins from only one race and expanded orthogroups were those containing more
243 proteins from a specific race than other races. Venn diagrams were created with the VennDiagram R
244 package version 1.6.20 (Chen and Boutros, 2011) in R version 3.2.5 (R Core Team, 2016).

245 Identification and analysis of variant sites and population structure

246 Variant sites were identified through the use of the GATK version 3.6 HaplotypeCaller in diploid
247 mode (McKenna et al., 2010) following alignment of Illumina reads for all sequenced isolates to the
248 FALCON-Unzip assembled genome with Bowtie 2 version 2.2.6 (Langmead and Salzberg, 2012) and
249 filtered with vcflib (Garrison, 2012) and VCFTools (Danecek et al., 2011). Additionally, structural
250 variants were identified with SvABA (Wala et al., 2018) following the alignment of Illumina reads
251 from all sequenced isolates to the FALCON-Unzip assembled genome with BWA-mem version 0.7.15
252 (Li, 2013). Population structure was assessed with fastSTRUCTURE (Raj et al., 2014) following
253 conversion of the input file with Plink version 1.90 beta (Purcell et al., 2007). Finally, a custom Python
254 script was used to identify variant sites private to races UK1, UK2 or UK3 (see Availability of
255 Computer Code below).

256 Assessment of gene expression levels and the identification of candidate avirulence 257 genes

258 RNA-Seq reads of BC-1, BC-16 and NOV-9 were aligned to the assembled genomes of BC-1, BC-16
259 and NOV-9 as described above. Expression levels and differentially expressed genes were identified
260 with featureCounts version 1.5.2 (Liao et al., 2014) and the DESeq2 version 1.10.1 R package (Love
261 et al., 2014). Multiple test correction was performed as part of the analysis within the DESeq2
262 package.

263 Candidate avirulence genes were identified through the analysis of uniquely expressed genes
264 and uniquely differentially expressed genes for each of the three isolates. Uniquely expressed genes
265 were those with a Fragments Per Kilobase of transcript per Million mapped reads (FPKM) value
266 greater than or equal to 5 in any time point from the inoculation time course experiment for a single
267 isolate. Uniquely differentially expressed genes were those with a minimum LFC of 3 and a *p*-value
268 threshold of 0.05. Genes were compared between isolates through the use of orthology group
269 assignments described above and scored on a one to six scale, with five and six deemed high
270 confidence and one and two deemed as low confidence.

271 To identify homologous genes in other *Phytophthora* spp., candidate RxLRs were processed
272 by SignalP-5.0 (Armenteros et al., 2019) to identify the cleavage site. The signal peptide sequence
273 was removed before being submitted for a tblastn (Altschul et al., 1997) search on GenBank;
274 interesting top hits are reported.

275 The expression levels of a strong candidate *PfAvr2* gene, PF003_g27513 and a candidate
276 *PfAvr3* gene, PF009_g26276, were assessed via RT-qPCR. RNA-Seq results for reference genes
277 identified previously in *Phytophthora parasitica* (Yan and Liou, 2006) were examined for stability of
278 expression levels, resulting in the selection of β-tubulin (PF003_g4288) and WS41 (PF003_g28439)
279 as reference genes. Primers were designed using the modified Primer3 version 2.3.7 implemented in
280 Geneious R10 (Untergasser et al., 2012). Reverse transcription was performed on three biological
281 replicates of each sequenced timepoint, alongside: 24 hpi, 72 hpi and 96 hpi for BC-1 and 24 hpi, 48
282 hpi and 96 hpi for NOV-9 with the QuantiTect Reverse Transcription Kit. Quantitative PCR (qPCR)
283 was then performed in a CFX96™ Real-Time PCR detection system in 10 µL reactions of: 5 µL of
284 2x qPCRBIO SyGreen Mix Lo-Rox, 2 µL of a 1:3 dilution of the cDNA sample in dH_2O and 0.4 µL
285 of each 10 µM primer and 2.2 µL dH_2O. The reaction was run with the following conditions: 95 °C
286 for 3 minutes, 39 cycles of 95 °C for 10 seconds, 62 °C for 10 seconds and 72 °C for 30 seconds. This
287 was followed by 95 °C for 10 seconds, and a 5 second step ranging from 65 °C to 95 °C by 0.5 °C
288 every cycle. At least two technical replicates for each sample were performed and the melt curve
289 results were analysed to ensure the correct product was detected. Relative gene expression was
290 calculated using the comparative cycle threshold (C_T) method (Livak and Schmittgen, 2001). Where
291 there was a difference of at least 1 C_T value between the minimum and maximum results for technical
292 replicates, further reactions were conducted. Outlier technical replicates were first identified as being
293 outside 1.5 times the interquartile range. Following this, additional outliers were identified using the
294 Grubb's test and excluded from the analysis. Technical replicates were averaged for each biological
295 replicate and expression values were calculated as the mean of the three biological replicates.

296 Investigation of *cis* and *trans* variations for strong candidate avirulence gene

297 The regions upstream and downstream of PF003_g27513 and PF009_g26276 in the FALCON-Unzip
298 assembly of BC-16 and the SMARTdenovo assembly of NOV-9 were aligned with MAFFT in
299 Geneious R10 (Katoh et al., 2002; Katoh and Standley, 2013). Variant sites were identified through
300 visual inspection of the alignment alongside visualisation of aligned short reads from BC-16 and

301 NOV-9 to both assemblies with Bowtie 2 version 2.2.6 (Langmead and Salzberg, 2012) in IGV
302 (Thorvaldsdóttir et al., 2013).
303 Transcription factors were identified with a previously described HMM of transcription factors
304 and transcriptional regulators in Stramenopiles (Buitrago-Flórez et al., 2014). These proteins were
305 then analysed through methods described above for gene loss or gain, nearby variant sites and
306 differential expression between isolates.

307 Availability of computer code

308 All computer code is available at:
309 https://github.com/harrisonlab/phytophthora_fragariae,
310 https://github.com/harrisonlab/phytophthora_rubi and
311 https://github.com/harrisonlab/popgen/blob/master/snp/vcf_find_difference_pop.py.
312

313 RESULTS

314 Race typing allowed standardisation of US and UK race nomenclature

315 The *P. fragariae* isolates A4 (race US4), BC-1 (race CA1), BC-16 (race CA3), NOV-5 (race CA1),
316 NOV-9 (race CA2), NOV-27 (race CA2) and NOV-71 (race CA2) (**Table 1**) were phenotyped on a
317 differential series of four *F.* × *ananassa* cultivars with known resistance. These were: 'Allstar'
318 (containing *Rpf1*, *Rpf2* and *Rpf3*), 'Cambridge Vigour' (containing *Rpf2* and *Rpf3*), 'Hapil'
319 (containing no resistance genes) and 'Redgauntlet' (containing *Rpf2*) (van de Weg et al., 1996; R.
320 Harrison, unpublished). Following assessment of below ground symptoms, it was shown that race
321 CA1 was equivalent to UK1, race CA2 was equivalent to UK3, race CA3 was equivalent to UK2 and
322 race US4 was equivalent to UK2 (**Figure 1; Table 2**).

323 A highly contiguous genome assembly of BC-16

324 Long read PacBio sequencing generated a highly contiguous *P. fragariae* isolate BC-16 (UK2)
325 reference genome of 91 Mb in 180 contigs with an N50 value of 923.5 kb (**Table 3**). This was slightly
326 larger than the closely related, well studied species from Clade 7, *P. sojae*, at 83 Mb (**Table 3**; Tyler
327 et al., 2006). The BC-16 assembly contained 266 of 303 eukaryotic Benchmarking Universal Single-
328 Copy Orthologs (BUSCO) genes (**Table 4**), compared to 270 in *P. sojae* (Armitage et al., 2018) and
329 so likely represented a similar completeness of the genome as the *P. sojae* assembly. The *P. fragariae*

330 genome was shown to be highly repeat rich, with 38% of the assembly identified as repetitive or low
331 complexity, a larger value than the 29% shown for *P. sojae* (Armitage et al., 2018). A total of 37,049
332 genes encoding 37,346 proteins were predicted in the BC-16 assembly, consistening of 20,222 genes
333 predicted by BRAKER1 (Hoff et al., 2016) and 17,131 additional genes added from CodingQuarry
334 (Testa et al., 2015). From these gene models, 486 putative RxLR effectors, 82 putatitve crinkler
335 effectors (CRNs) and 1,274 putative apoplastic effectors were identified (**Table 5**). Additionally, a
336 total of 4,054 low confidence gene models were added from intergenic ORFs identified as putative
337 effectors. These consisted of 566 putative RxLRs, 5 putative CRNs and 3,483 putatitve apoplastic
338 effectors. This resulted in a combined total of 41,103 genes encoding 41,400 proteins with 1,052
339 putative RxLRs, 85 putative CRNs and 4,757 putative apoplastic effectors (**Table 3** and **Table 5**).

340 **A comparable number of effector genes were identified through resequencing of isolates of**
341 ***Phytophthora fragariae* and *Phytophthora rubi***

342 Ten isolates of *P. fragariae* and three isolates of *P. rubi* were additionally resequenced, *de novo*
343 assembled and annotated (**Table 1** and **Table 4**). These isolates showed similar assembly statistics
344 within and between species; an average of 79 Mb in 12,804 contigs with an N50 of 19.3 kb in *P.*
345 *fragariae*, compared to an average of 78 Mb in 13,882 contigs with an N50 of 16.8 kb in *P. rubi*. All
346 assemblies showed 31% of the assembly was identified as repetitive or low complexity sequences. On
347 average both *P. fragariae* and *P. rubi* showed high levels of completeness, with an average of 274/303
348 BUSCO genes identified as single copies in these assemblies. Interestingly, a total of 17 genes were
349 consistently not identified in Illumina, PacBio and Nanopore assemblies of *P. fragariae* and *P. rubi*
350 isolates, suggesting these genes may be absent from these species and as such may not be considered
351 true eukaryotic BUSCO genes. An average of 67 CRNs were predicted in *P. fragariae* and an average
352 of 118 CRNs in *P. rubi*. A significantly (p = 0.013) smaller number of RxLRs were predicted in *P.*
353 *rubi* isolates than *P. fragariae* isolates alongside a significantly (p = 0.039) smaller number of
354 apoplastic effectors predicted in *P. rubi* than *P. fragariae* (**Table 5**). However, it is important to note
355 that these effectors were predicted from a subset of secreted proteins, of which there were significantly
356 (p = 0.030) fewer predicted in *P. rubi* than in *P. fragariae* (**Table 5**).

357 **No distinguishing gene loss or gain; or the presence of INDELs or SNPs in candidate avirulence**
358 **genes could be found associated with race variation**

359 An orthology analysis of all predicted proteins from the isolates of *P. fragariae* and *P. rubi* assigned
360 481,942 (98.7%) proteins to 38,891 orthogroups. Of these groups, 17,101 contained at least one
361 protein from all fourteen sequenced isolates and 13,132 of these groups consisted entirely of single-
362 copy proteins from each isolate. There were 2,345 of these groups unique to *P. rubi* and 1,911 of these
363 groups unique to *P. fragariae*. Analysis of unique and expanded orthogroups for isolates of the UK1,
364 UK2 and UK3 races did not lead to the identification of candidate avirulence genes, as these groups
365 did not contain putative effector genes (**Figure 2**).

366 A total of 725,444 SNP sites and 95,478 small INDELs were identified within the *P. fragariae*
367 and *P. rubi* isolates by the Genome Analysis ToolKit (GATK) haplotypecaller (McKenna et al., 2010)
368 and 80,388 indels and 7,020 structural variants were identified by SvABA (Wala et al., 2018).
369 Analysis of high quality, biallelic SNP sites allowed the identification of a distinct population
370 consisting of the isolates of race UK1, UK2 and UK3, hereafter referred to as the UK1-2-3 population,
371 with SCRP245, the only UK isolate, potentially forming an ancestral or hybrid isolate between the
372 UK1-2-3 population and the population represented by BC-23 and ONT-3 (**Figure 3; Supplementary**
373 **Figure S2**). Additionally, clear separation between isolates of *P. fragariae* and *P. rubi* was observed.
374 Further analysis within the UK1-2-3 population allowed for the identification of private variants,
375 which were only present in isolates of one of the three races in this population. This resulted in the
376 identification of eleven private variants in the UK2 race shared between both A4 and BC-16; however,
377 neither the genes they fell within or were neighbours to were predicted to encode effectors or secreted
378 proteins and likely did not explain the differences in pathogenicity.

379 **Wide scale transcriptional reprogramming of effectors during strawberry infection**

380 RNA-Seq data were generated from an inoculation time course experiment for representatives of races
381 UK1, UK2 and UK3; BC-1, BC-16 and NOV-9 respectively. Following determination of expression
382 levels of the predicted genes in both *in planta* and mycelia samples, a correlation analysis showed
383 biological replicates of each timepoint grouped together (**Figure 4**). Additionally, the 48 hours post
384 inoculation (hpi) BC-1 time point grouped with the BC-16 24 hpi time point, suggesting these may
385 represent similar points in the infection process. However, clear separation between the BC-16
386 timepoints was observed (**Figure 4**). A total of 13,240 transcripts from BC-16 (32%) showed
387 expression above a FPKM value threshold of five in at least one sequenced BC-16 time point and

388 9,329 (23%) of these showed evidence of differential expression in at least one sequenced *in planta*
389 time point compared to mycelium grown in artificial media, suggesting large scale transcriptional
390 reprogramming. As three time points post inoculation were sequenced for BC-16, the changes in
391 expression over the course of the infection process was investigated. A total of 2,321 transcripts (6%)
392 showed a Log_2 Fold Change (LFC) greater than or equal to one or less than or equal to minus one,
393 representing a general reprofiling during infection in comparison to growth in artificial media. Of
394 transcripts differentially expressed *in planta* compared to artificial media, fewer transcripts were
395 differentially expressed at both 24 hpi and 96 hpi than between sequential timepoints (297 compared
396 to 1,016 and 1,604 transcripts). This suggested that changes during the progress of infection were
397 captured by this dataset (**Figure 5**).
398 Levels of expression of effector genes were also assessed. A total of 274 (26%) RxLR
399 effectors, 27 (31%) CRNs and 880 (18%) putative apoplastic effectors from BC-16 showed evidence
400 of expression above the FPKM threshold of 5 in at least one sequenced time point. The majority of
401 these effector genes also showed evidence of differential expression during *in planta* time points
402 compared to *in vitro* mycelium. A total of 253 (24%) RxLR effectors, 19 (22%) CRNs and 888 (18%)
403 putative apoplastic effectors showed an LFC greater than or equal to one or less than or equal to minus
404 one, representing wide scale transcriptional reprogramming of effector genes during infection (**Figure**
405 **5**). Ranking of the 50 highest expressed genes *in planta* with a LFC of ≥3 in comparison to its
406 respective mycelium, identified four putative RxLR genes that were upregulated by all three isolates
407 (**Table 6**). These genes represent putative core *P. fragariae* RxLR's important for pathogenicity on
408 strawberry. Interestingly, a BLASTP search of one of these putative core effectors, PF003_g16448
409 (amino acids 19-139), showed homology to *P. sojae Avr1b* (58 % pairwise identity), GenBank
410 accession AF449625 (Shan et al., 2004).

411 **RxLR effector PF003_g27513 is a strong candidate for *PfAvr2***

412 Comparing transcripts with the highest LFC (*in planta* vs mycelium) between isolates led to the
413 identification of the putative RxLR effector encoding transcript PF003_g27513.t1 as a potential
414 candidate for *PfAvr2* in BC-16. PF003_g27513 had a peak FPKM value in BC-16 of 9,392 compared
415 to peaks of 5 and 34, in BC-1 and NOV-9, respectively (**Supplementary Table S2**). Subsequent RT-
416 qPCR analysis of further timepoints in the *in planta* timecourse supported the findings of the RNA-
417 Seq timepoints and showed the expression of putative *PfAvr2* in the UK2 isolates BC-16 and A4 was
418 significantly ($p < 0.05$) different to those from all samples of BC-1 (UK1) and NOV-9 (UK3; **Figure**

419 **6**). A BLASTP search of PF003_g16448 (amino acids 26-137) revealed homology to *P. sojae*
420 *Avh6/Avr1d* (37 % pairwise identity), GenBank accession JN253642 (Wang et al., 2011; Na et al.,
421 2013).

422 The surrounding sequence of putative *PfAvr2* in BC-16, BC-1 and NOV-9 was investigated
423 for sequence variants that may explain the expression difference. As no variants were identified near
424 the gene from the above mentioned variant panel, an assembly of the NOV-9 isolate was created from
425 Nanopore sequencing data, producing an assembly of 93.72 Mbp in 124 contigs with an N50 of 1,260
426 Kb. This resulted in the identification of a SNP from T in BC-16 to G in NOV-9 ~14 Kb downstream
427 of the stop codon and a 30 bp insertion in NOV-9 ~19 Kb upstream of the start codon (**Figure 7A**).
428 The upstream variant appeared to be a sequencing error following the investigation of the alignment
429 of short reads of BC-16 and NOV-9 to each assembly and so was rejected. Expression of the genes
430 surrounding PF003_g27513 was investigated and PF003_g27514, directly upstream of putative
431 *PfAvr2* is expressed by all three isolates (**Supplementary Table S2**).

432 Additionally, putative transcription factors and transcriptional regulators were identified in all
433 sequenced genomes. This resulted in the identification of 269 genes in the BC-16 isolate of *P.*
434 *fragariae*. However, analysis of gene loss or gain and an investigation of variant sites showed no race
435 specific differences, though expression level variation was observed.

436 **RxLR effector PF009_g26276 is a putative candidate for *PfAvr3***

437 Further analysis of the RNA-Seq datasets identified the putative RxLR effector encoding transcript
438 PF009_g26276 (an orthologue of PF003_g27386) as a potential candidate for *PfAvr3* in NOV-9, with
439 a peak FPKM value in NOV-9 of 199 compared to *in planta* peaks of 6 and 12 in BC-1 and BC-16,
440 respectively (**Supplementary Table S3**). Similar to putative *PfAvr2*, no sequence differences in
441 putative *PfAvr3* were observed between the three isolates. Analysis of the surrounding region between
442 NOV-9 and BC-16 showed no sequence differences 13,000 bp upstream and 3,761 bp downstream of
443 PF009_g26276 (**Figure 7B**). The two genes upstream from putative *PfAvr3* are not expressed in any
444 isolate (**Supplementary Table S3**), whereas the gene directly downstream in BC-16, PF003_g27385,
445 is expressed by all the three isolates analysed.

446 Subsequent RT-qPCR analysis of further timepoints in the *in planta* time course revealed that
447 the putative *PfAvr3* was not expressed during any timepoints by the UK1 isolate BC-1 or by the UK2
448 isolates BC-16 and A4 (**Supplementary Figure S3**). However, absolute expression of

449 PF009_g26276 in NOV-9 remained low. Expression in NOV-9 at 72 hpi was significantly ($p < 0.05$)
450 greater than those from all samples of BC-1, BC-16 and A4.

451 **Candidate genes for *PfAvr1* identified from expression level variation**

452 Analysis of the RNA-Seq datasets did not reveal an obvious candidate for *PfAvr1*. Further analysis
453 using custom scripts identified genes, which were uniquely expressed in BC-1 and those uniquely
454 differentially expressed. These genes were scored for confidence of race avirulence determinant; high,
455 medium and low. No genes were identified in the high confidence class in BC-1, but four genes were
456 scored as medium confidence, one of which was a putative apoplastic effector (**Supporting**
457 **Candidate Table**). The analysis was repeated for BC-16 and NOV-9, in case the putative RxLR
458 candidates are not *PfAvr*2 and *PfAvr3*, respectively (**Supporting Candidate Table**).
459

460 # DISCUSSION

461 Understanding pathogenicity of plant pathogens is critical for developing durable resistance strategies.
462 *P. fragariae* is a continuing threat to strawberry production. The UK1-2-3 population displayed clear
463 separation from the other isolates of *P. fragariae* in this study. Two putative avirulence candidates for
464 UK2 and UK3 were identified through population resequencing and analyses of gene expression
465 during *P. fragariae* infection. We have shown that there are no distinguishing gene loss or gain events,
466 INDELs or SNPs associated with race variation in UK1-2-3. Our results also suggest that the
467 polymorphisms associated with avirulence to race UK2 and UK3 resistance is controlled *in trans* or
468 with other stable forms of epigenetic modulating gene expression.

469 This study utilised long read sequencing technologies to improve the contiguity of the *P.*
470 *fragariae* genome through the assembly of a greater amount of repeat rich sequence. Though this
471 assembly still fell short of the estimated chromosome number of 10 - 12 (Brasier et al., 1999), at 180
472 contigs, it is a significant improvement over the previous assemblies that utilised solely short read
473 technologies and produced relatively fragmented assemblies, comprised of >1,000 contigs each (Gao
474 et al., 2015; Tabima et al., 2017). The increase in size of the assembly presented (91 Mb), suggests
475 that the assembly includes an increased amount of repetitive sequence, indicating that it represents a
476 more complete genome assembly than previous attempts. Although the assembly presented here was
477 larger than previously reported assemblies, it is similar in size to the related Clade 7b species *P. sojae*
478 (95 Mb; Tyler et al., 2006). This study produced assemblies of an additional ten isolates of *P. fragariae*
479 and three isolates of the closely related raspberry pathogen *P. rubi* with short read technology. These

480 assemblies were of similar sizes and contiguity to those previously published (Gao et al., 2015;
481 Tabima et al., 2017).

482 All assemblies produced from PacBio and Illumina sequencing were annotated and putative
483 effector genes were predicted. The gene model totals are likely inflated, due to the use of a greedy
484 approach to effector gene prediction, to ensure the capture of all possible virulence genes. ApoplastP
485 appeared to over-predict effectors, likely due to statistical issues arising from the use of a training set
486 far smaller than the query set used in this study (Pritchard and Broadhurst, 2014). Interestingly, twice
487 as many CRNs were predicted in *P. rubi* than *P. fragariae* on average (average of 118 in *P. rubi* and
488 67 in *P. fragariae*), though this was not consistent for all *P. rubi* isolates. In comparison to *P. sojae*,
489 the BC-16 isolate was predicted to possess approximately 50% more RxLRs and twice as many CRNs
490 from RNA-Seq guided gene models (Tyler et al., 2006). This difference may have been due to
491 improvements in prediction strategies, as the number of CRNs was similar to those predicted for the
492 Clade 1 species *P. cactorum* (Armitage et al., 2018). However for RxLR effectors this difference is
493 likely explained by the greedy approach taken for gene prediction in this study. Following the
494 validation of gene models by RNA-Seq data, the likely overprediction of effector genes was also
495 shown by the low percentage of these classes of genes showing evidence of expression.

496 This work also allowed the resolution of *P. fragariae* race schemes between different
497 countries, Canadian race 1 is equivalent to UK race 1, Canadian race 2 is equivalent to UK race 3 and
498 both Canadian race 3 and USA race 4 is equivalent to UK race 2. This provided further support for
499 the proposed gene-for-gene model of resistance in this pathosystem (van de Weg, 1997a). However,
500 construction of orthology groups for all isolates of *P. fragariae* and *P. rubi* did not show the presence
501 of proteins unique to the races UK1, UK2 and UK3. Additionally, the identification of variant sites,
502 with the BC-16 genome acting as a reference, indicated there were only private variants present in
503 UK2, with none identified in UK1 or UK3. None of these variants were in proximity to genes thought
504 to be involved in pathogenicity. Additionally, analysis of population structure confirmed the
505 previously described species separation of *P. fragariae* and *P. rubi* (Man in 't Veld, 2007; Tabima et
506 al., 2018) and identified a subpopulation consisting of the isolates of *P. fragariae* of UK1-2-3 on
507 which further investigations focused.

508 Transcriptome analyses led to the identification of a strong candidate for *PfAvr2*, which was
509 shown to be highly expressed in all *in planta* BC-16 timepoints, compared to evidence of no, or very
510 low levels of expression in any BC-1 (UK1) or NOV-9 (UK3) samples. The strongest candidate for
511 *PfAvr3* was also shown to be differentially expressed between races, but not as highly expressed in

512 NOV-9 as observed for putative *PfAvr2*. RT-qPCR confirmed the *PfAvr2* results and additionally
513 showed expression of *PfAvr2* in the other sequenced UK2 isolate, A4. The assay showed high levels
514 of variability, which was due to variation between biological replicates, likely the result of the inability
515 of the inoculation method to control the quantity of zoospores inoculating an individual plant. Further
516 *in planta* experiments and RT-qPCR of additional isolates are required to investigate the observations
517 of putative *PfAvr3*.

518 We propose that silencing of putative *PfAvr2* in races UK1 and UK3, enables those isolates to
519 evade recognition in *Rpf2* possessing plants, such as 'Redgauntlet', but not in plants possessing '*Rpf1*'
520 or '*Rpf3*', respectively. Silencing of putative *PfAvr3* also enables races UK1 and UK2 to evade
521 recognition in *Rpf3* possessing plants, as long as they also do not possess *Rpf1* and *Rpf3*.

522 Whilst the exact mechanism of putative *PfAvr2* and *PfAvr3* silencing was not identified in this
523 study, long read sequencing of a race UK3 isolate (NOV-9) identified a single SNP, 14 kb downstream
524 of the stop codon of putative *PfAvr2* and variation in expression of transcription factors was observed
525 in the RNA-Seq data. This indicated that epigenetic modifications could explain the observed
526 transcriptional variation. Transcriptional silencing of effectors is a known mechanism that
527 *Phytophthora* spp. employ to evade the activation of host *R*-gene-mediated immunity. Investigations
528 of the EC-1 clonal lineage of *P. infestans* revealed a variation of the ability of isolates to cause disease
529 on potato plants possessing the *Rpi-vnt1.1* gene. It was shown, in the absence of genetic mutations,
530 that differences in the expression level of *Avrvnt1* were detected that correlated with virulence (Pais
531 et al., 2018). Recent work in *P. infestans* and *P. sojae* has shown evidence of adenine N6-methylation
532 (6mA) alongside a lack of evidence of 5-methylcytosine (5mC) DNA methylation, highlighting that
533 6mA methylation is an important epigenetic mark for the regulation of gene expression in
534 *Phytophthora* spp. (Chen et al., 2018). It is also possible that chromatin modifications may be involved
535 in controlling the expression differences, as demonstrated in *P. infestans* (van West et al., 2008; Chen
536 et al., 2018). Investigation of these possibilities, while not achievable in the current study is a clear
537 direction for future research.

538 Nearly all *P. fragariae* isolates investigated in this study were collected from around Canada
539 between 2001-2012. The SCRP245 isolate was identified as an intermediate between the UK1-2-3
540 population and the population represented by the BC-23 and ONT-3 isolates. SCRP245 could
541 represent a rare hybrid of the two populations. However, due to the small sample size of isolates, the
542 low number of SNP sites available for this analysis and the fact it was isolated in 1945 in the UK, at
543 least 55 years before the other isolates, it appears more likely that SCRP245 represents a separate

544 population but the data available were unable to resolve this fully. Further race typing with differential
545 strawberry genotypes is required to ascertain the relationship between isolates of Canadian races 4
546 and 5.

547 Races of asexual species have been shown to evolve by the stepwise accumulation of
548 mutations (Del Mar Jiménez-Gasco et al., 2004). One such example is the successive evolution of
549 multiple pathotypes in a single clonal lineage of the wheat pathogen *Puccinia striiformis* f. sp. *tritici*
550 in Australia and New Zealand (Steele et al., 2001). In comparison, our data do not indicate that *P.*
551 *fragariae* has undergone simple stepwise evolution of effectors, but we rather postulate that some
552 lineages of *P. fragariae* have been present for long periods of time in nature, evident by the large
553 number of SNP differences and well supported branches and that the emergence of races (e.g. UK1-
554 2-3) is fairly recent, possibly as a result of the *R*-genes deployed in commercial strawberries. The
555 increased selection pressure on *P. fragariae* to overcome these genes, or the break-up of 'wild' R
556 gene stacks upon hybridisation of octoploid strawberry species, may have led to very rapid evolution
557 of races, in this case through epigenetic silencing of gene expression, to evade the *R*-genes present in
558 common cultivars. Substantial further sampling from multiple geographic regions would be required
559 to fully decipher population structure in the lineages of *P. fragariae* and the resistance status of wild
560 octoploid *Fragaria* species. We predict that this would lead to the observation of other geographically
561 distinct lineages of genetically similar individuals of *P. fragariae* but with similar differences in
562 pathogenicity on strawberry. The implications of these findings highlight the potential adaptability of
563 *P. fragariae* to modify effector expression to evade host resistance and the threat of the emergence of
564 new races. Future strawberry breeding efforts must deploy cultivars with multiple resistance genes to
565 mitigate against the rapid adaptation of *P. fragariae*. Identifying resistance genes that recognise the
566 conserved core RxLRs identified in this study would enable broad-spectrum resistance to this
567 pathogen to be deployed that would be effective against multiple races. One of the conserved highly
568 expressed RxLRs was shown to have homology to *P. sojae Avr1b* and so identifying homologous *R*-
569 genes to *Rsp1b* in strawberry could be a future avenue of work to provide resistance against multiple
570 races.

571 In conclusion, we have shown for the first time that within a distinct subpopulation of *P.*
572 *fragariae* isolates, displaying remarkably low levels of polymorphisms, the ability to cause disease on
573 a range of differing strawberry cultivars was controlled by variation in transcriptional levels rather
574 than being due to sequence variation, similar to reports in *P. infestans* (Pais et al., 2018). This study
575 presents a large amount of data, including an improved, long read assembly of *P. fragariae* alongside

576 a collection of resequenced isolates of *P. fragariae* and *P. rubi*, and transcriptome data from multiple
577 isolates that is a valuable resource for future studies.
578

579 ## AUTHOR CONTRIBUTIONS

580 RH, CN and TA devised the study. RH, CN and JD co-supervised TA's PhD study, within which
581 some of this work was undertaken. TA performed the experimental work, with contributions from
582 CN. AA assisted with the development of genome assembly, annotation and orthology pipelines. MS
583 developed elements of the variant calling pipeline and structure analysis with TA. HB performed
584 Nanopore and MiSeq sequencing. JT, BK, BT and NG provided RNA-Seq reads of *P. rubi* for genome
585 annotation. TA drafted the manuscript with input from CN, JD and RH. All authors read and approved
586 the submission.
587

588 ## FUNDING

589 This research was supported by grants awarded from the Biotechnology and Biological Sciences
590 Research Council (BBSRC) to RH (BB/K017071/1, BB/K017071/2 and BB/N006682/1) and Sophien
591 Kamoun (BB/K018639/1).
592

593 ## ACKNOWLEDGEMENTS

594 The authors gratefully acknowledge the East Malling Strawberry Breeding Club for access to
595 strawberry material, to Dr. Andrew R. Jamieson for the *P. fragariae* isolates as well as Dr. David E.L.
596 Cooke for the *P. rubi* isolates and *P. fragariae* SCRP245. The authors also gratefully acknowledge
597 Prof. Sophien Kamoun, Dr. Eric van de Weg and Dr. Thijs van Dijk for useful discussions. In addition,
598 we wish to thank the following people for the help received in the preparation and setting up of
599 experiments Dr. Helen M. Cockerton, Dr. Laura A. Lewis and Mr. Joseph Hutchings, as well as the
600 members of RH's group. Work was carried out under the terms of DEFRA Plant Health Licence
601 6996/221427 held by RH/CN.
602

603 ## DATA AVAILABILITY STATEMENT

604 The datasets, including all assemblies and annotations, generated for this study are available on NCBI
605 GenBank as part of BioProjects PRJNA396163 and PRJNA488213 with accession numbers of
606 SAMN07449679 - SAMN07449692. Raw sequencing reads have been deposited in the NCBI SRA,

607 DNA-Seq reads are available with accession codes SRR7668085 - SRR7668100 and *P. fragariae*
608 RNA-Seq reads are available with accession codes SRR7764607 - SRR7764615. *P. rubi* RNA-Seq
609 reads are available with the accession codes SRR10207404 - SRR10207405.
610
611

612 **REFERENCES**

613 Adams, T. M. (2019). Pathogenomics of *Phytophthora fragariae*, the causal agent of strawberry red
614 core disease [PhD thesis]. [Reading (UK)]: University of Reading.

615 Altschul, S. F., Madden, T. L., Schäffer, A. A., Zhang, J., Zhang, Z., Miller, W., and Lipman, D. J.
616 (1997). Gapped BLAST and PSI-BLAST: a new generation of protein database search
617 programs. *Nucleic Acids Res*. 25, 3389-3402.

618 Armenteros, J. J. A., Tsirigos, K. D., Sønderby, C. K., Petersen, T. N., Winther, O., Brunak, S., et al.
619 (2019). SignalP 5.0 improves signal peptide predictions using deep neural networks. *Nat.*
620 *Biotechnol.* 37, 420–423. doi.org/10.1038/s41587-019-0036-z.

621 Armitage, A. D., Lysøe, E., Nellist, C. F., Lewis, L. A., Cano, L. M., Harrison, R. J., et al. (2018).
622 Bioinformatic characterisation of the effector repertoire of the strawberry pathogen
623 *Phytophthora cactorum*. *PLoS ONE* 13, e0202305. doi:10.1371/journal.pone.0202305.

624 Aronesty, E. (2013). Comparison of Sequencing Utility Programs. *Open Bioinforma. J.* 7, 1–8.
625 doi:10.2174/1875036201307010001.

626 Bankevich, A., Nurk, S., Antipov, D., Gurevich, A. A., Dvorkin, M., Kulikov, A. S., et al. (2012).
627 SPAdes: a new genome assembly algorithm and its applications to single-cell sequencing. *J.*
628 *Comput. Biol.* 19, 455–477. doi:10.1089/cmb.2012.0021.

629 Bendtsen, J. D., Nielsen, H., von Heijne, G. and Brunak, S. (2004) Improved Prediction of Signal
630 Peptides: SignalP 3.0. *J. Mol. Biol*. **340**(4), 783-795. doi:10.1016/j.jmb.2004.05.028.

631 Brasier, C. M., Cooke, D. E., and Duncan, J. M. (1999). Origin of a new Phytophthora pathogen
632 through interspecific hybridization. *Proc Natl Acad Sci USA* 96, 5878–5883.
633 doi:10.1073/pnas.96.10.5878.

634 Buitrago-Flórez, F. J., Restrepo, S., and Riaño-Pachón, D. M. (2014). Identification of transcription
635 factor genes and their correlation with the high diversity of stramenopiles. *PLoS ONE* 9,
636 e111841. doi:10.1371/journal.pone.0111841.

637 Campbell, A. M., Moon, R. P., Duncan, J. M., Gurr, S.-J., and Kinghorn, J. R. (1989). Protoplast
638 formation and regeneration from sporangia and encysted zoospores of *Phytophthora infestans*.
639 *Physiol. Mol. Plant P.* 34, 299–307. doi:10.1016/0885-5765(89)90027-1.

640 Clifford, R. J., Milillo, M., Prestwood, J., Quintero, R., Zurawski, D. V., Kwak, Y. I., et al. (2012)
641 Detection of Bacterial 16S rRNA and Identification of Four Clinically Important Bacteria by
642 Real-Time PCR. *PLoS ONE* 7, e48558. doi:10.1371/journal.pone.0048558

643 Chen, H., and Boutros, P. C. (2011). VennDiagram: a package for the generation of highly-
644 customizable Venn and Euler diagrams in R. *BMC Bioinformatics* 12, 35. doi:10.1186/1471-
645 2105-12-35.

646 Chen, H., Shu, H., Wang, L., Zhang, F., Li, X., Ochola, S. O., et al. (2018). Phytophthora
647 methylomes are modulated by 6mA methyltransferases and associated with adaptive genome
648 regions. *Genome Biol.* 19, 181. doi:10.1186/s13059-018-1564-4.

649 Chin, C.-S., Alexander, D. H., Marks, P., Klammer, A. A., Drake, J., Heiner, C., et al. (2013).
650 Nonhybrid, finished microbial genome assemblies from long-read SMRT sequencing data. *Nat.*
651 *Methods* 10, 563–569. doi:10.1038/nmeth.2474.

652 Chin, C.-S., Peluso, P., Sedlazeck, F. J., Nattestad, M., Concepcion, G. T., Clum, A., et al. (2016).
653 Phased diploid genome assembly with single-molecule real-time sequencing. *Nat. Methods* 13,
654 1050–1054. doi:10.1038/nmeth.4035.

655 Cui, C., Herlihy, J., Bombarely, A., McDowell, J. M., and Haak, D. C. (2019). Draft assembly of
656 *Phytopthora capsici* from long-read sequencing uncovers complexity. *Mol. Plant Microbe*
657 *Interact.* doi:10.1094/MPMI-04-19-0103-TA.

658 Danecek, P., Auton, A., Abecasis, G., Albers, C. A., Banks, E., DePristo, M. A., et al. (2011). The
659 variant call format and VCFtools. *Bioinformatics* 27, 2156–2158.
660 doi:10.1093/bioinformatics/btr330.

661 Del Mar Jiménez-Gasco, M., Milgroom, M. G., and Jiménez-Díaz, R. M. (2004). Stepwise Evolution
662 of Races in *Fusarium oxysporum* f. sp. *ciceris* Inferred from Fingerprinting with Repetitive
663 DNA Sequences. *Phytopathology* 94, 228–235. doi:10.1094/PHYTO.2004.94.3.228.

664 Dobin, A., Davis, C. A., Schlesinger, F., Drenkow, J., Zaleski, C., Jha, S., et al. (2013). STAR:
665 ultrafast universal RNA-seq aligner. *Bioinformatics* 29, 15–21.
666 doi:10.1093/bioinformatics/bts635.

667 Dong, S., Qutob, D., Tedman-Jones, J., Kuflu, K., Wang, Y., Tyler, B. M., et al. (2009). The
668 *Phytophthora sojae* avirulence locus Avr3c encodes a multi-copy RXLR effector with sequence
669 polymorphisms among pathogen strains. *PLoS ONE* 4, e5556.
670 doi:10.1371/journal.pone.0005556.

671 EFSA Panel on Plant Health (PLH) (2014). Scientific Opinion on the risks to plant health posed by
672 *Phytophthora fragariae* Hickman var. *fragariae* in the EU territory, with the identification and
673 evaluation of risk reduction options. *EFSA Journal* 12. doi:10.2903/j.efsa.2014.3539.

674 Emms, D. M., and Kelly, S. (2015). OrthoFinder: solving fundamental biases in whole genome
675 comparisons dramatically improves orthogroup inference accuracy. *Genome Biol.* 16, 157.
676 doi:10.1186/s13059-015-0721-2.

677 EPPO (2018). EPPO A2 List. *EPPO A2 List*. Available at:
678 https://www.eppo.int/ACTIVITIES/plant_quarantine/A2_list [Accessed January 31, 2019].

679 Gao, R., Cheng, Y., Wang, Y., Wang, Y., Guo, L., and Zhang, G. (2015). Genome Sequence of
680 *Phytophthora fragariae* var. *fragariae*, a Quarantine Plant-Pathogenic Fungus. *Genome*
681 *Announc.* 3. doi:10.1128/genomeA.00034-15.

682 Garrison, E. (2012). *Vcflib. A C++ library for parsing and manipulating VCF files*. Github
683 Available at: https://github.com/ekg/vcflib [Accessed December 19, 2018].

684 Gurevich, A., Saveliev, V., Vyahhi, N., and Tesler, G. (2013). QUAST: quality assessment tool for
685 genome assemblies. *Bioinformatics* 29, 1072–1075. doi:10.1093/bioinformatics/btt086.

686 Haas, B. (2010). *TransposonPSI: an application of PSI-blast to mine (Retro-)transposon ORF*
687 *homologies.* sourceforge Available at: http://transposonpsi.sourceforge.net/ [Accessed January
688 10, 2019].

689 Hickman, C. J. (1941). The Red Core Root Disease of The Strawberry Caused By *Phytophthora*
690 *Fragariae* n.sp. *Journal of Pomology and Horticultural Science* 18, 89–118.
691 doi:10.1080/03683621.1941.11513556.

692 Hoff, K. J., Lange, S., Lomsadze, A., Borodovsky, M., and Stanke, M. (2016). BRAKER1:
693 Unsupervised RNA-Seq-Based Genome Annotation with GeneMark-ET and AUGUSTUS.
694 *Bioinformatics* 32, 767–769. doi:10.1093/bioinformatics/btv661.

695 Judelson, H. S., Coffey, M. D., Arredondo, F. R., and Tyler, B. M. (1993). Transformation of the
696 oomycete pathogen *Phytophthora megasperma* f. sp. *glycinea* occurs by DNA integration into
697 single or multiple chromosomes. *Curr. Genet.* 23, 211–218. doi:10.1007/BF00351498.

698 Käll L., Krogh, A. and Sonnhammer, E. L. L. (2004). A Combined Transmembrane Topology and
699 Signal Peptide Prediction Method. *J. Mol. Biol*. 338(5), 1027-1036.
700 doi:10.1016/j.jmb.2004.03.016.

701 Katoh, K., Misawa, K., Kuma, K., and Miyata, T. (2002). MAFFT: a novel method for rapid
702 multiple sequence alignment based on fast Fourier transform. *Nucleic Acids Res.* 30, 3059–
703 3066. doi:10.1093/nar/gkf436.

704 Katoh, K., and Standley, D. M. (2013). MAFFT multiple sequence alignment software version 7:
705 improvements in performance and usability. *Mol. Biol. Evol.* 30, 772–780.
706 doi:10.1093/molbev/mst010.

707 Koren, S., Walenz, B. P., Berlin, K., Miller, J. R., Bergman, N. H., and Phillippy, A. M. (2017).
708 Canu: scalable and accurate long-read assembly via adaptive k-mer weighting and repeat
709 separation. *Genome Res.* 27, 722–736. doi:10.1101/gr.215087.116.

710 Langmead, B., and Salzberg, S. L. (2012). Fast gapped-read alignment with Bowtie 2. *Nat. Methods*
711 9, 357–359. doi:10.1038/nmeth.1923.

712 Liao, Y., Smyth, G. K., and Shi, W. (2014). featureCounts: an efficient general purpose program for
713 assigning sequence reads to genomic features. *Bioinformatics* 30, 923–930.
714 doi:10.1093/bioinformatics/btt656.

715 Livak, K. J., and Schmittgen, T. D. (2001). Analysis of relative gene expression data using real-time
716 quantitative PCR and the 2(-Delta Delta C(T)) Method. *Methods* 25, 402–408.
717 doi:10.1006/meth.2001.1262.

718 Li, H. (2013). Aligning sequence reads, clone sequences and assembly contigs with BWA-MEM.
719 *arXiv*.

720 Li, H. (2018). Minimap2: pairwise alignment for nucleotide sequences. *Bioinformatics* 34, 3094–
721 3100. doi:10.1093/bioinformatics/bty191.

722 Li, H., Handsaker, B., Wysoker, A., Fennell, T., Ruan, J., Homer, et al. (2009). The Sequence
723 Alignment/Map format and SAMtools. *Bioinformatics* 25, 2078–2079.
724 doi:10.1093/bioinformatics/btp352.

725 Love, M. I., Huber, W., and Anders, S. (2014). Moderated estimation of fold change and dispersion
726 for RNA-seq data with DESeq2. *Genome Biol.* 15, 550. doi:10.1186/s13059-014-0550-8.

727 Maas, J. L. (1972). Growth and reproduction in culture of ten *Phytophthora fragariae* races.
728 *Mycopathol. Mycol. Appl.* 48, 323–334. doi:10.1007/BF02052636.

729 Malar C, M., Yuzon, J. D., Das, S., Das, A., Panda, A., Ghosh, S., et al. (2019). Haplotype-Phased
730 Genome Assembly of Virulent *Phytophthora ramorum* Isolate ND886 Facilitated by Long-
731 Read Sequencing Reveals Effector Polymorphisms and Copy Number Variation. *Mol. Plant*
732 *Microbe Interact.* 32, 1047–1060. doi:10.1094/MPMI-08-18-0222-R.

733 Man in ’t Veld, W. A. (2007). Gene flow analysis demonstrates that *Phytophthora fragariae* var.*rubi*
734 constitutes a distinct species, *Phytophthora rubi* comb. nov. *Mycologia* 99, 222–226.
735 doi:10.1080/15572536.2007.11832581.

736 McKenna, A., Hanna, M., Banks, E., Sivachenko, A., Cibulskis, K., Kernytsky, A., et al. (2010). The
737 Genome Analysis Toolkit: a MapReduce framework for analyzing next-generation DNA
738 sequencing data. *Genome Res.* 20, 1297–1303. doi:10.1101/gr.107524.110.

739 Na, R., Yu, D., Qutob, D., Zhao, J., and Gijzen, M. (2013). Deletion of the *Phytophthora sojae*
740 avirulence gene *Avr1d* causes gain of virulence on *Rsp1d*. *Mol. Plant Microbe Interact.* 26(6),
741 969–976. doi.org/10.1094/MPMI-02-13-0036-R.

742 Nielsen, H., Englebrecht, J., Brunak S. and von Heijne G. (1997). Identification of prokaryotic and
743 eukaryotic signal peptides and prediction of their cleavage sites. *Protein Eng.* 10(1), 1-6.
744 doi:10.1093/protein/10.1.1.

745 Pais, M., Yoshida, K., Giannakopoulou, A., Pel, M. A., Cano, L. M., Oliva, R. F., et al. (2018). Gene
746 expression polymorphism underpins evasion of host immunity in an asexual lineage of the Irish
747 potato famine pathogen. *BMC Evol. Biol.* 18, 93. doi:10.1186/s12862-018-1201-6.

748 Petersen, T. N., Brunak, S., Heijne, von, G., & Nielsen, H. (2011). SignalP 4.0: discriminating signal
749 peptides from transmembrane regions. *Nat. Methods*, 8, 785–786. doi:10.1038/nmeth.1701.

750 van Poppel, P. M. J. A., Guo, J., van de Vondervoort, P. J. I., Jung, M. W. M., Birch, P. R. J.,
751 Whisson, S. C., et al. (2008). The *Phytophthora infestans* avirulence gene Avr4 encodes an
752 RXLR-dEER effector. *Mol. Plant Microbe Interact.* 21, 1460–1470. doi:10.1094/MPMI-21-11-
753 1460.

754 Pritchard, L., and Broadhurst, D. (2014). On the statistics of identifying candidate pathogen
755 effectors. *Methods Mol. Biol.* 1127, 53–64. doi:10.1007/978-1-62703-986-4_4.

756 Purcell, S., Neale, B., Todd-Brown, K., Thomas, L., Ferreira, M. A. R., Bender, D., et al. (2007).
757 PLINK: a tool set for whole-genome association and population-based linkage analyses. *Am. J.*
758 *Hum. Genet.* 81, 559–575. doi:10.1086/519795.

759 Raj, A., Stephens, M., and Pritchard, J. K. (2014). fastSTRUCTURE: variational inference of
760 population structure in large SNP data sets. *Genetics* 197, 573–589.
761 doi:10.1534/genetics.114.164350.

762 Robinson Boyer, L., Feng, W., Gulbis, N., Hajdu, K., Harrison, R. J., Jeffries, P., et al. (2016). The
763 use of arbuscular mycorrhizal fungi to improve strawberry production in coir substrate. *Front.*
764 *Plant. Sci*. 7, 1237. doi:10.3389/fpls.2016.01237.

765 Ruan, J. (2018). *SMARTdenovo: Ultra-fast de novo assembler using long noisy reads.* Github
766 Available at: https://github.com/ruanjue/smartdenovo [Accessed January 10, 2019].

767 R Core Team (2016). *R: A Language and Environment for Statistical Computing*. R Foundation for
768 Statistical Computing, Vienna, Austria Available at: https://www.R-project.org [Accessed
769 December 19, 2018].

770 R core team (2017). *R: A language and environment for statistical computing.* R Foundation for
771 Statistical Computing, Vienna, Austria Available at: https://www.R-project.org [Accessed
772 December 19, 2018].

773 Shan, W., Cao, M., Leung, D., & Tyler, B. M. (2004). The *Avr1b* locus of *Phytophthora sojae*
774 encodes an elicitor and a regulator required for avirulence on soybean plants carrying resistance
775 gene *Rps1b*. *Mol. Plant Microbe Interact.* 17(4), 394–403. doi: 10.1094/MPMI.2004.17.4.394.

776 Shulaev, V., Sargent, D. J., Crowhurst, R. N., Mockler, T. C., Folkerts, O., Delcher, et al. (2011).
777 The genome of woodland strawberry (*Fragaria vesca*). *Nat. Genet.* 43, 109–116.
778 doi:10.1038/ng.740.

779 Simão, F. A., Waterhouse, R. M., Ioannidis, P., Kriventseva, E. V., and Zdobnov, E. M. (2015).
780 BUSCO: assessing genome assembly and annotation completeness with single-copy orthologs.
781 *Bioinformatics* 31, 3210–3212. doi:10.1093/bioinformatics/btv351.

782 Simpson, J. (2018). *Nanopolish: Signal-level algorithms for MinION data*. Github Available at:
783 https://github.com/jts/nanopolish [Accessed January 10, 2019].

784 Smit, A. F. A., and Hubley, R. (2015). *RepeatModeler Open-1.0*. Repeatmasker.org Available at:
785 http://www.repeatmasker.org [Accessed January 10, 2019].

786 Smit, A. F. A., Hubley, R., and Green, P. (2015). *RepeatMasker Open-4.0*. repeatmasker.org
787 Available at: http://www.repeatmasker.org [Accessed January 10, 2019].

788 Sperschneider, J., Dodds, P. N., Singh, K. B., and Taylor, J. M. (2018). ApoplastP: prediction of
789 effectors and plant proteins in the apoplast using machine learning. *New Phytol.* 217, 1764–
790 1778. doi:10.1111/nph.14946.

791 Steele, K. A., Humphreys, E., Wellings, C. R., and Dickinson, M. J. (2001). Support for a stepwise
792 mutation model for pathogen evolution in Australasian *Puccinia striiformis* f.sp. *tritici* by use of
793 molecular markers. *Plant Pathology* 50, 174–180. doi:10.1046/j.1365-3059.2001.00558.x.

794 Tabima, J. F., Coffey, M. D., Zazada, I. A., and Grünwald, N. J. (2018). Populations of
795 *Phytophthora rubi* Show Little Differentiation and High Rates of Migration Among States in
796 the Western United States. *Mol. Plant Microbe Interact.* 31, 614–622. doi:10.1094/MPMI-10-
797 17-0258-R.

798 Tabima, J. F., Kronmiller, B. A., Press, C. M., Tyler, B. M., Zasada, I. A., and Grünwald, N. J.
799 (2017). Whole Genome Sequences of the Raspberry and Strawberry Pathogens *Phytophthora*
800 *rubi* and *P. fragariae*. *Mol. Plant Microbe Interact.* 30, 767–769. doi:10.1094/MPMI-04-17-
801 0081-A.

802 Taylor, A., Vágány, V., Jackson, A. C., Harrison, R. J., Rainoni, A., and Clarkson, J. P. (2016).
803 Identification of pathogenicity-related genes in *Fusarium oxysporum* f. sp. *cepae. Mol. Plant*
804 *Pathol.* 17, 1032–1047. doi:10.1111/mpp.12346.

805 Testa, A. C., Hane, J. K., Ellwood, S. R., and Oliver, R. P. (2015). CodingQuarry: highly accurate
806 hidden Markov model gene prediction in fungal genomes using RNA-seq transcripts. *BMC*
807 *Genomics* 16, 170. doi:10.1186/s12864-015-1344-4.

808 Thorvaldsdóttir, H., Robinson, J. T., and Mesirov, J. P. (2013). Integrative Genomics Viewer (IGV):
809 high-performance genomics data visualization and exploration. *Brief. Bioinformatics* 14, 178–
810 192. doi:10.1093/bib/bbs017.

811 Tyler, B. M., Tripathy, S., Zhang, X., Dehal, P., Jiang, R. H. Y., Aerts, A., et al. (2006).
812 Phytophthora genome sequences uncover evolutionary origins and mechanisms of pathogenesis.
813 *Science* 313, 1261–1266. doi:10.1126/science.1128796.

814 Untergasser, A., Cutcutache, I., Koressaar, T., Ye, J., Faircloth, B. C., Remm, M., et al. (2012).
815 Primer3--new capabilities and interfaces. *Nucleic Acids Res.* 40, e115. doi:10.1093/nar/gks596.

816 Vaser, R., Sović, I., Nagarajan, N., and Šikić, M. (2017). Fast and accurate de novo genome
817 assembly from long uncorrected reads. *Genome Res.* 27, 737–746. doi:10.1101/gr.214270.116.

818 Wala, J. A., Bandopadhayay, P., Greenwald, N. F., O'Rourke, R., Sharpe, T., Stewart, C., et al.
819 (2018). SvABA: genome-wide detection of structural variants and indels by local assembly.
820 *Genome Res.* 28, 581–591. doi:10.1101/gr.221028.117.

821 Walker, B. J., Abeel, T., Shea, T., Priest, M., Abouelliel, A., Sakthikumar, S., et al. (2014). Pilon: an
822 integrated tool for comprehensive microbial variant detection and genome assembly
823 improvement. *PLoS ONE* 9, e112963. doi:10.1371/journal.pone.0112963.

824 van de Weg, W. E. (1997a). A gene-for-gene model to explain interactions between cultivars of
825 strawberry and races of *Phytophthora fragariae* var. *fragariae*. *Theor. Appl. Genet.* 94, 445–
826 451. doi:10.1007/s001220050435.

827 van de Weg, W. E. (1997b). *Gene-for-gene relationships between strawberry and the causal agent of*
828 *red stele root rot,* Phytophthora fragariae *var.* fragariae.

829 van de Weg, W. E., Giezen, S., Henken, B., and den Nijs, A. P. M. (1996). A quantitative
830 classification method for assessing resistance to *Phytophthora fragariae* var. *fragariae* in
831 strawberry. *Euphytica* 91, 119–125. doi:10.1007/BF00035282.

832 van West, P., Shepherd, S. J., Walker, C. A., Li, S., Appiah, A. A., Grenville-Briggs, L. J., et al.
833 (2008). Internuclear gene silencing in *Phytophthora infestans* is established through chromatin
834 remodelling. *Microbiology* 154, 1482–1490. doi:10.1099/mic.0.2007/015545-0.

835 Wang, Q., Han, C., Ferreira, A. O., Yu, X., Ye, W., Tripathy, S., et al. (2011). Transcriptional
836 programming and functional interactions within the *Phytophthora sojae* RXLR effector
837 repertoire. *The Plant Cell*. 23(6), 2064–2086. doi.org/10.1105/tpc.111.086082.

838 Whisson, S. C., Boevink, P. C., Moleleki, L., Avrova, A. O., Morales, J. G., Gilroy, E. M., et al.
839 (2007). A translocation signal for delivery of oomycete effector proteins into host plant cells.
840 *Nature*. 450(7166), 115-118. doi:10.1038/nature06203.

841 Wickham, H. (2016). *ggplot2: Elegant Graphics for Data Analysis*. 2nd, illustrated ed. Springer.

842 Wick, R. (2018). *Porechop: adapter trimmer for Oxford Nanopore reads*. Github Available at:
843 https://github.com/rrwick/Porechop [Accessed January 9, 2019].

844 Wilcox, W. F., Scott, P. H., Hamm, P. B., Kennedy, D. M., Duncan, J. M., Brasier, C. M., et al.
845 (1993). Identity of a Phytophthora species attacking raspberry in Europe and North America.
846 *Mycol. Res.* 97, 817–831. doi:10.1016/S0953-7562(09)81157-X.

847 Yan, H.-Z., and Liou, R.-F. (2006). Selection of internal control genes for real-time quantitative RT-
848 PCR assays in the oomycete plant pathogen *Phytophthora parasitica*. *Fungal Genet. Biol.* 43,
849 430–438. doi:10.1016/j.fgb.2006.01.010.

850 Yin, W., Dong, S., Zhai, L., Lin, Y., Zheng, X., and Wang, Y. (2013). The *Phytophthora sojae*
851 Avr1d gene encodes an RxLR-dEER effector with presence and absence polymorphisms among
852 pathogen strains. *Mol. Plant Microbe Interact.* 26, 958–968. doi:10.1094/MPMI-02-13-0035-R.

853 Yu, D., Tang, H., Zhang, Y., Du, Z., Yu, H., and Chen, Q. (2012). Comparison and Improvement of
854 Different Methods of RNA Isolation from Strawberry (*Fragaria* × *ananassa*). *JAS* 4.
855 doi:10.5539/jas.v4n7p51.

856

857 **Conflict of Interest Statement:** The authors declare that the research was conducted in the absence
858 of any commercial or financial relationships that could be constructed as a potential conflict of
859 interest.

860

861

862

863 **FIGURES**

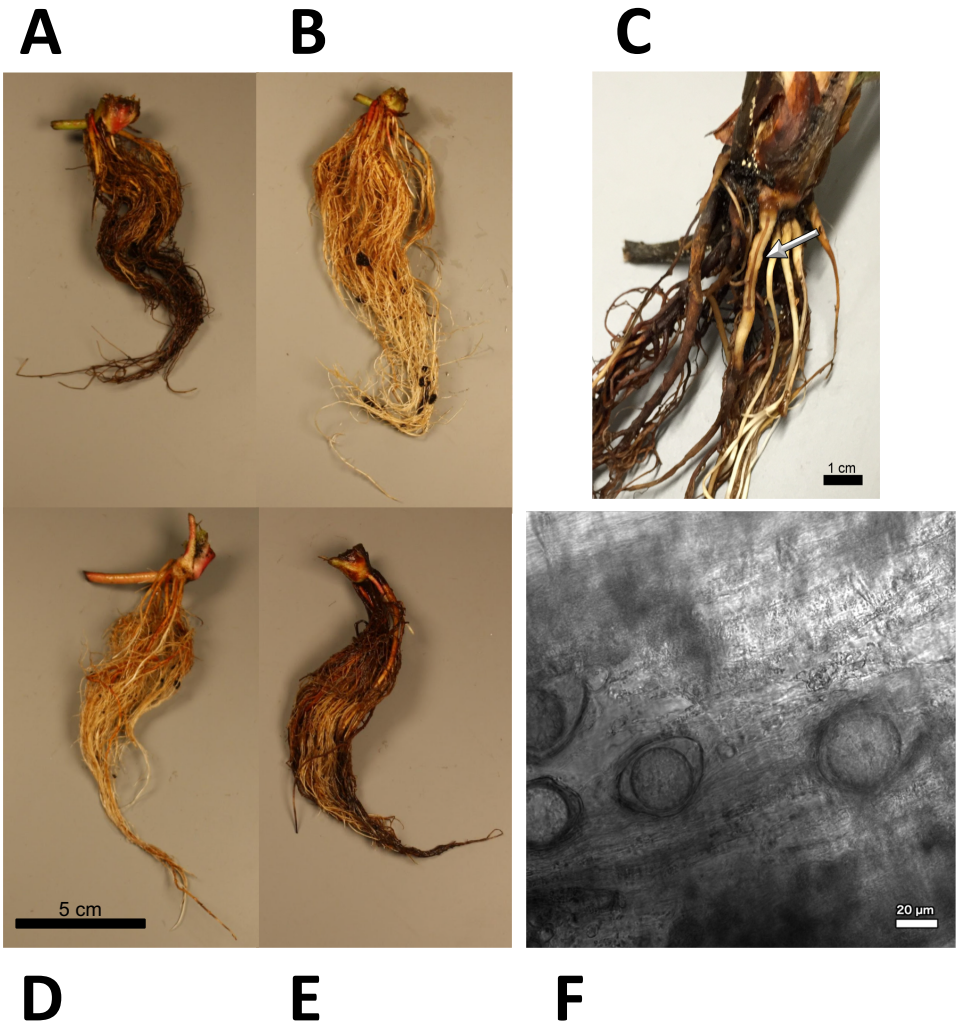

864

865 **FIGURE 1 | Observed *Phytophthora fragariae* symptoms in the cultivated strawberry (*Fragaria***
866 **× *ananassa*). (A,B,D,E)** Roots of *Fragaria* × *ananassa* harvested six weeks after inoculation with
867 *Phytophthora fragariae* mycelial slurry. **(A)** Successful infection of the *P. fragariae* isolate NOV-27
868 (race CA2) on a susceptible 'Redgauntlet' plant (*Rpf2* only). **(B)** Unsuccessful infection of the *P.*
869 *fragariae* isolate A4 (US4/UK2) on a resistant 'Redgauntlet' plant (*Rpf2* only). **(C)** Example of "red
870 core" symptoms observed in 'Hapil' roots infected with BC-16, three weeks post inoculation. **(D)**
871 Unsuccessful infection of the *P. fragariae* isolate NOV-27 (race CA2) on a resistant 'Allstar' plant
872 (*Rpf1*, *Rpf2* and *Rpf3*). **(E)** Successful infection of the *P. fragariae* isolate A4 (race US4/UK2) on a
873 susceptible 'Hapil' plant (no *Rpf* genes). **(F)** Example of BC-16 oospores observed in 'Hapil' roots, 3
874 weeks post inoculation, confirming infection.

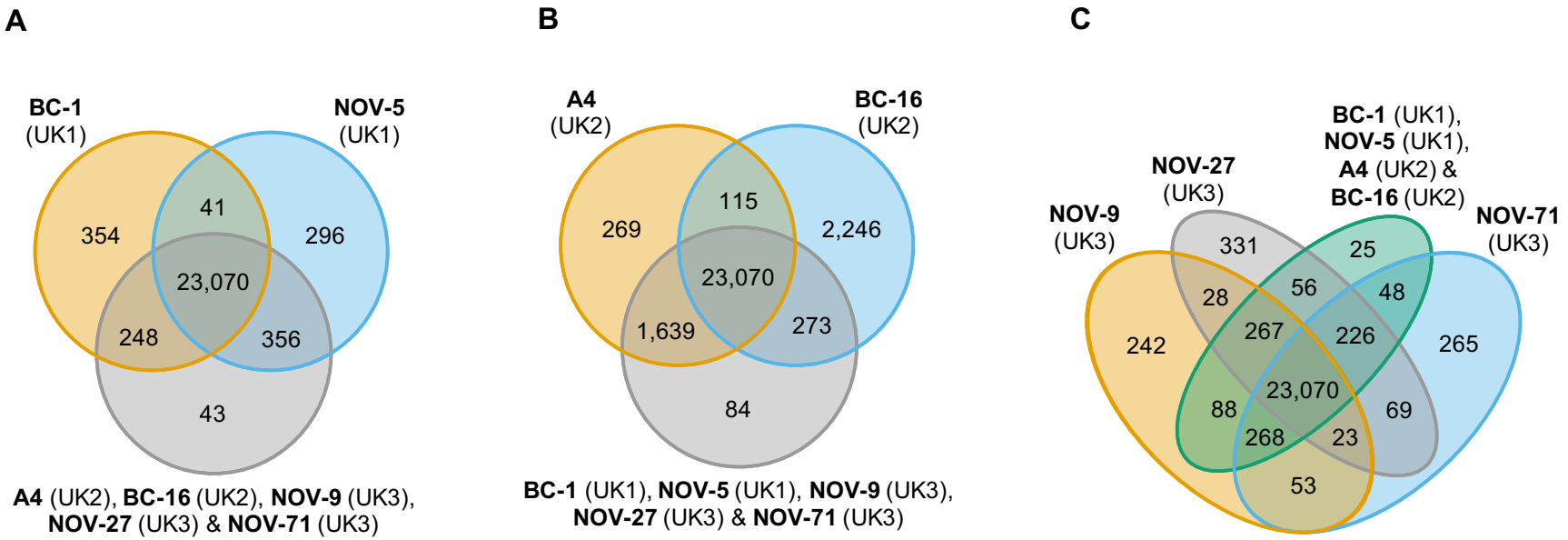

FIGURE 2 | Analysis of unique and expanded orthogroups for *Phytophthora fragariae* isolates of the UK1, UK2 and UK3 races did not lead to the identification of candidate avirulence genes. Orthology groups were identified by OrthoFinder (Emms and Kelly, 2015) and Venn diagrams were plotted using the VennDiagram R package (Chen and Boutros, 2011) in R (R Core Team, 2016). **(A)** Analysis focused on the *P. fragariae* isolates of race UK1: BC-1 and NOV-5 compared to isolates of races UK2 and UK3. **(B)** Analysis focused on the *P. fragariae* isolates of race UK2: A4 and BC-16 compared to isolates of races UK1 and UK3. **(C)** Analysis focused on the *P. fragariae* isolates of race UK3: NOV-5, NOV-27 and NOV-71 compared to isolates of races UK1 and UK2.

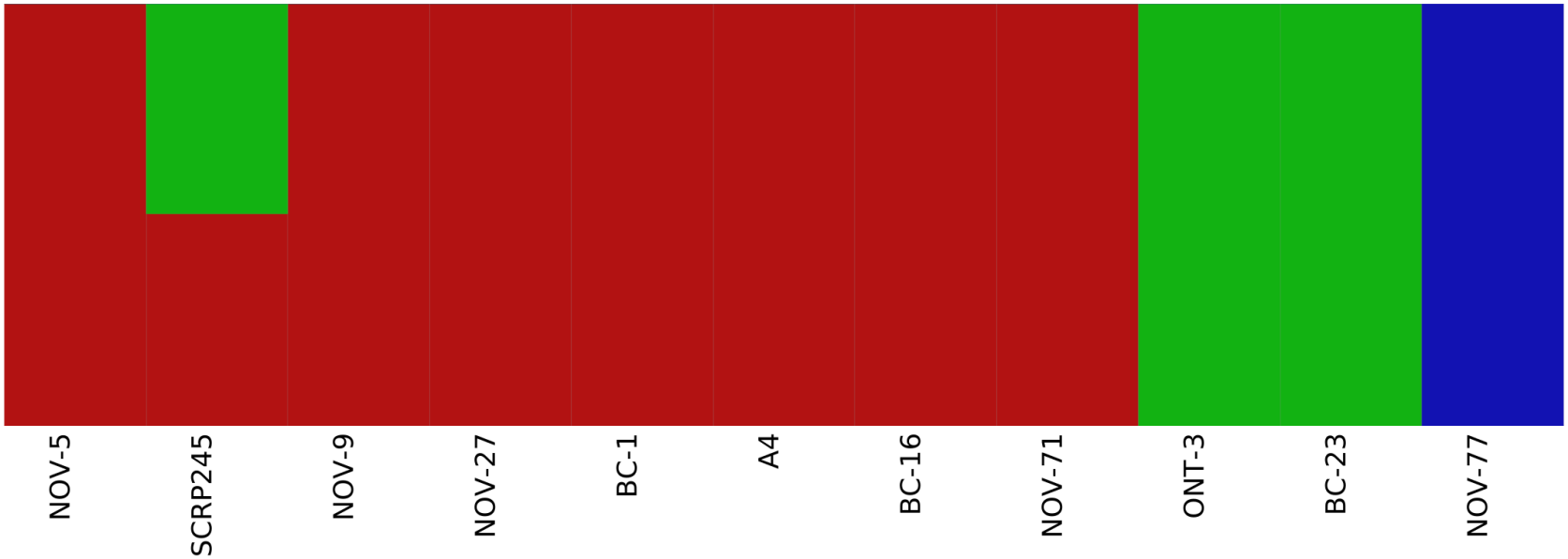

FIGURE 3 | Analysis of high quality, biallelic SNP sites split the isolates into three populations with SCRP245, potentially forming an ancestral or hybrid isolate between the UK1-2-3 population and the population represented by BC-23 and ONT-3. Distruct plot of fastSTRUCTURE (Raj et al., 2014) results carried out on all sequenced isolates of *Phytophthora fragariae*. Each colour represents a different population. Variant sites were identified by aligning Illumina reads of all the sequenced isolates to the reference assembly of the BC-16 isolate of *P. fragariae* with Bowtie 2 (Langmead and Salzberg, 2012) and analysis with the Genome Analysis Toolkit (GATK) haplotypecaller (McKenna et al., 2010). Sites were filtered with VCFtools (Danecek et al., 2011) and VCFlib (Garrison, 2012) to leave only high quality, biallelic SNP sites.

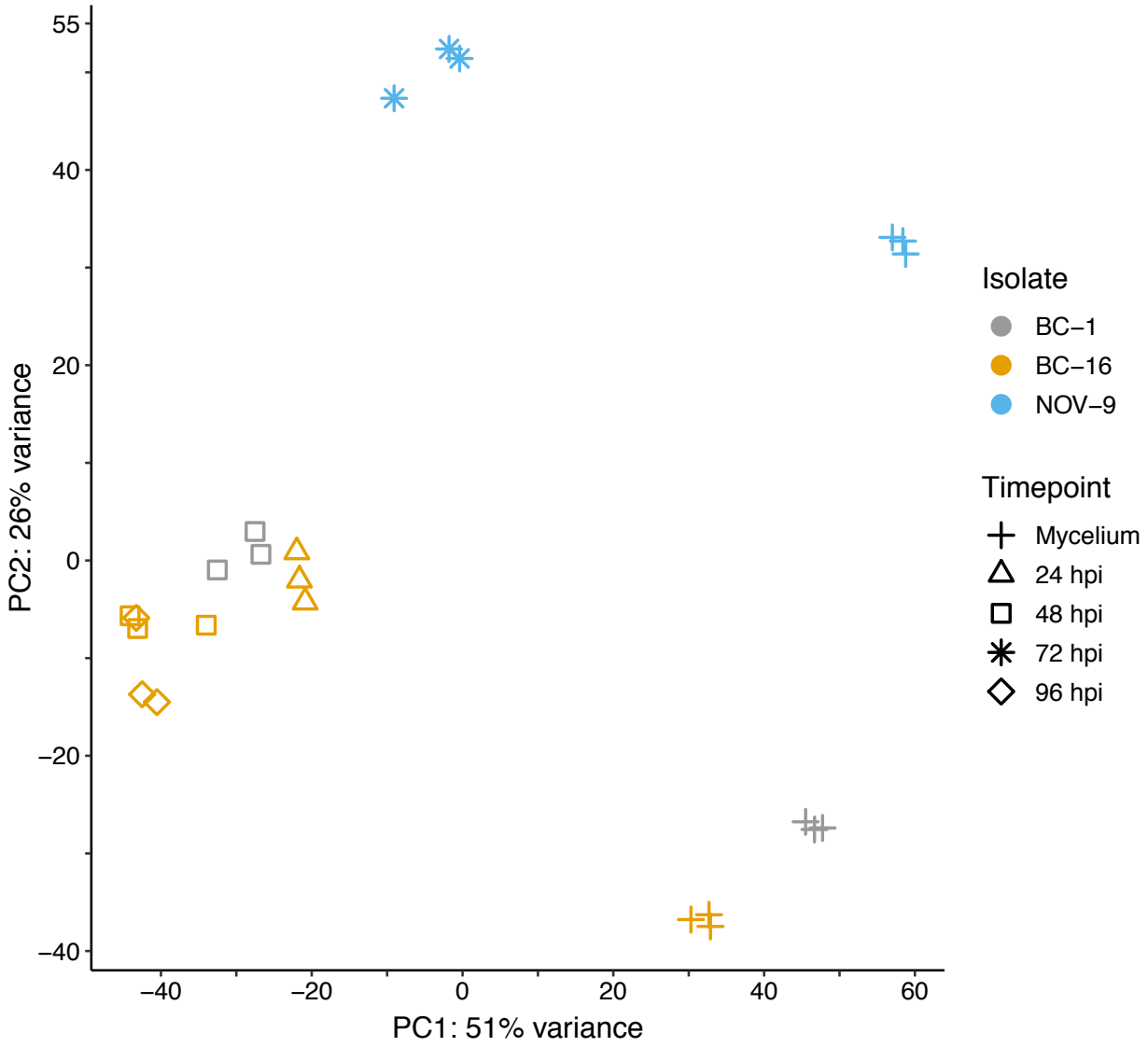

FIGURE 4 | Principal component analysis of expression data showed biological replicates of each timepoint grouped together, with clear separation observed for the BC-16 timepoints. RNA-Seq reads were aligned to the assembly of the BC-16 isolate of *Phytophthora fragariae* using STAR version 2.5.3a (Dobin et al., 2013). Predicted transcripts were then quantified with featureCounts version 1.5.2 (Liao et al., 2014) and differential expression was identified with the DESeq2 version 1.10.1 R package (Love et al., 2014). Following this, an rlog transformation of the expression data was plotted as a principal component analysis with R (R Core Team, 2016).

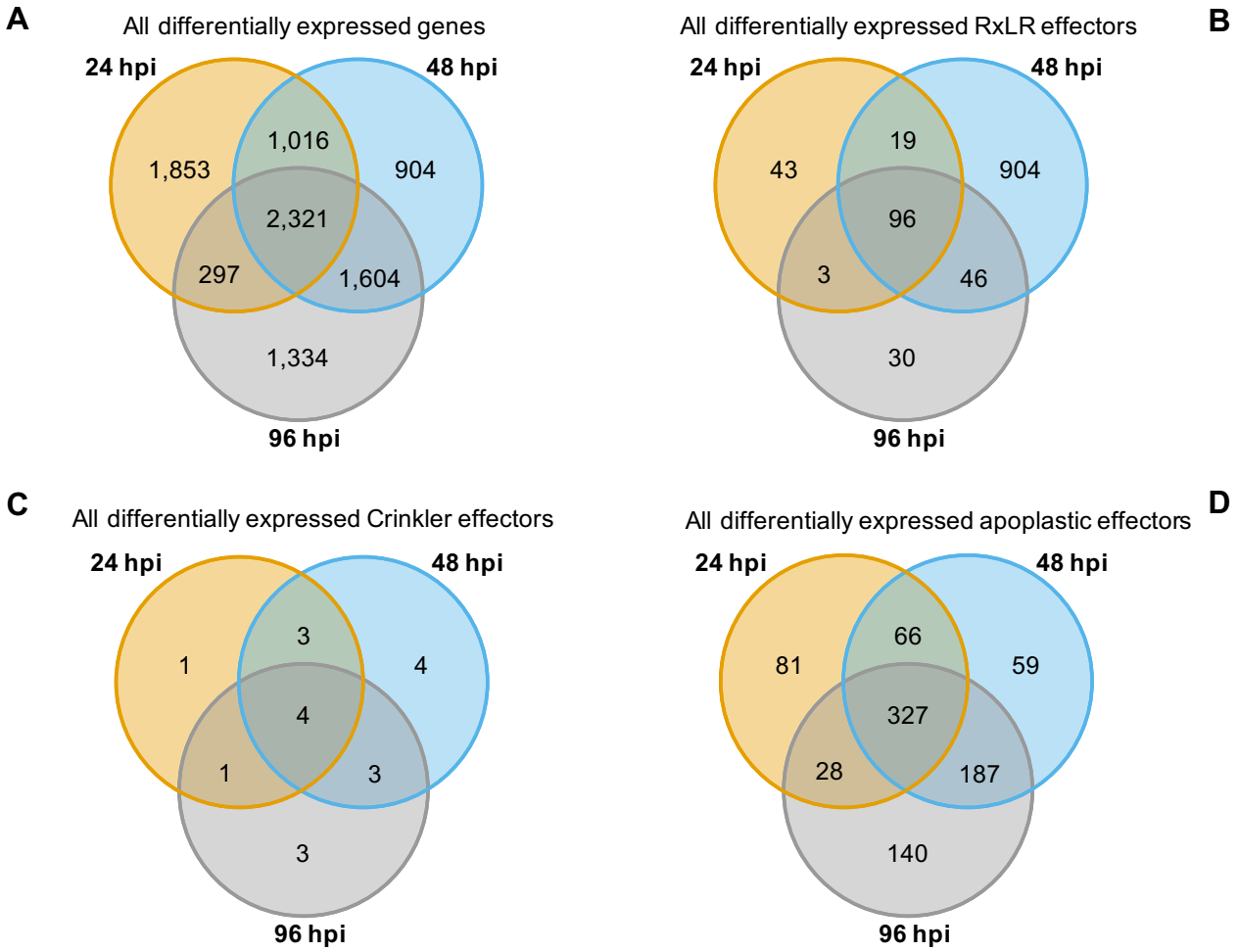

898

899 **FIGURE 5 | *In planta* RNA-Seq dataset captured changes during the progress of infection in the**
900 ***Phytophthora fragariae* BC-16 isolate.** RNA-Seq reads were aligned to the assembly of the BC-16
901 isolate of *P. fragariae* using STAR (Dobin et al., 2013). Predicted transcripts were then quantified
902 with featureCounts (Liao et al., 2014) and differential expression was identified with DESeq2 (Love
903 et al., 2014). Following this, Venn diagrams were plotted using the VennDiagram R package (Chen
904 and Boutros, 2011) in R (R Core Team, 2016). **(A)** All differentially expressed genes. **(B)** All
905 differentially expressed RxLR effectors. **(C)** All differentially expressed Crinkler effectors. **(D)** All
906 differentially expressed putative apoplastic effectors.

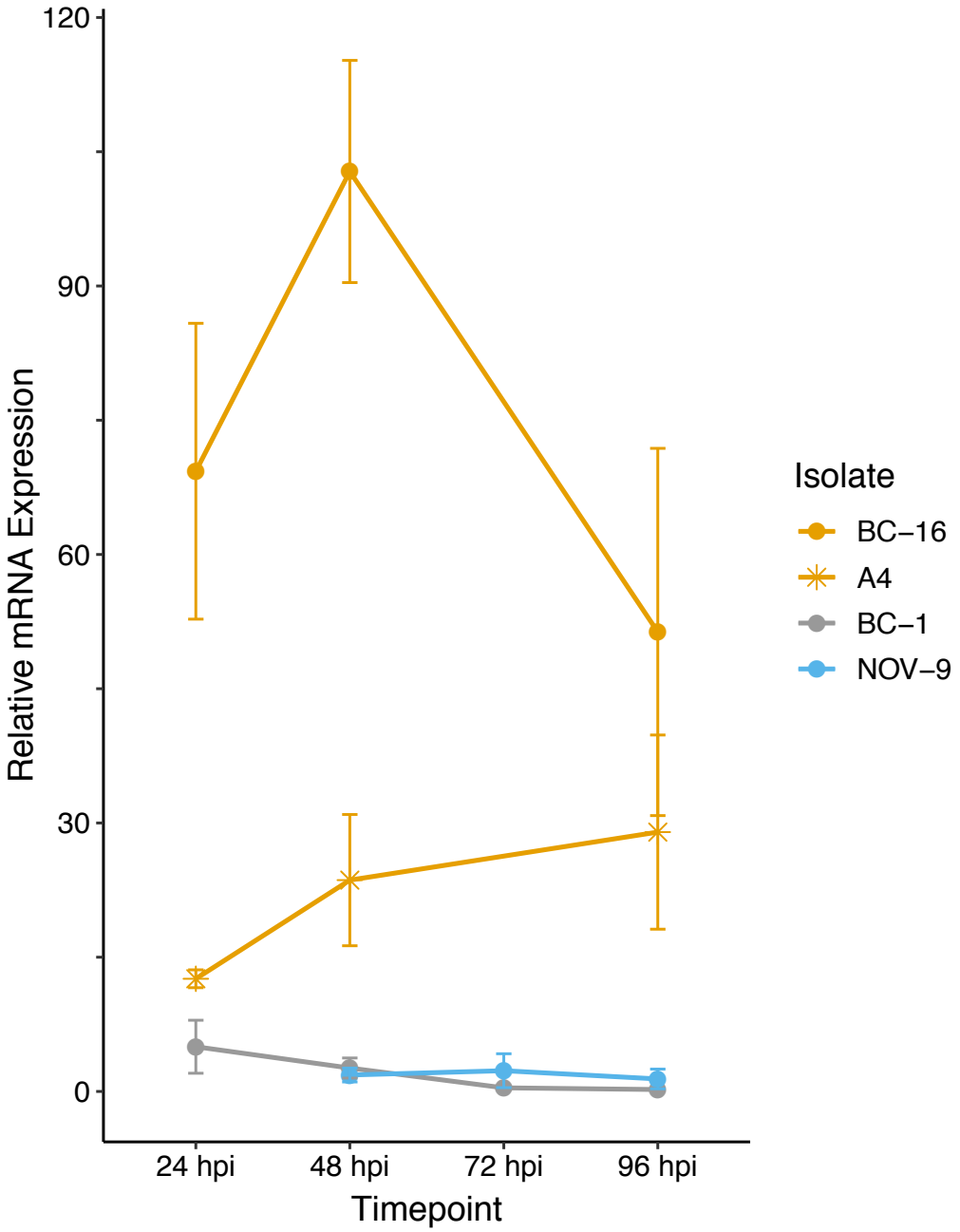

907

908 **FIGURE 6 | *PfAvr2* candidate PF003_g27513 is differentially expressed in *Phytophthora***
909 ***fragariae* UK-1-2-3 isolates.** Quantitative reverse transcription PCR of a strong candidate for the
910 avirulence gene possessed by BC-16 and A4, but not BC-1 and NOV-9 (PF003_g27513.t1). Plots
911 created by the ggplot2 R package (Wickham, 2016) in R version 3.4.3 (R core team, 2017).

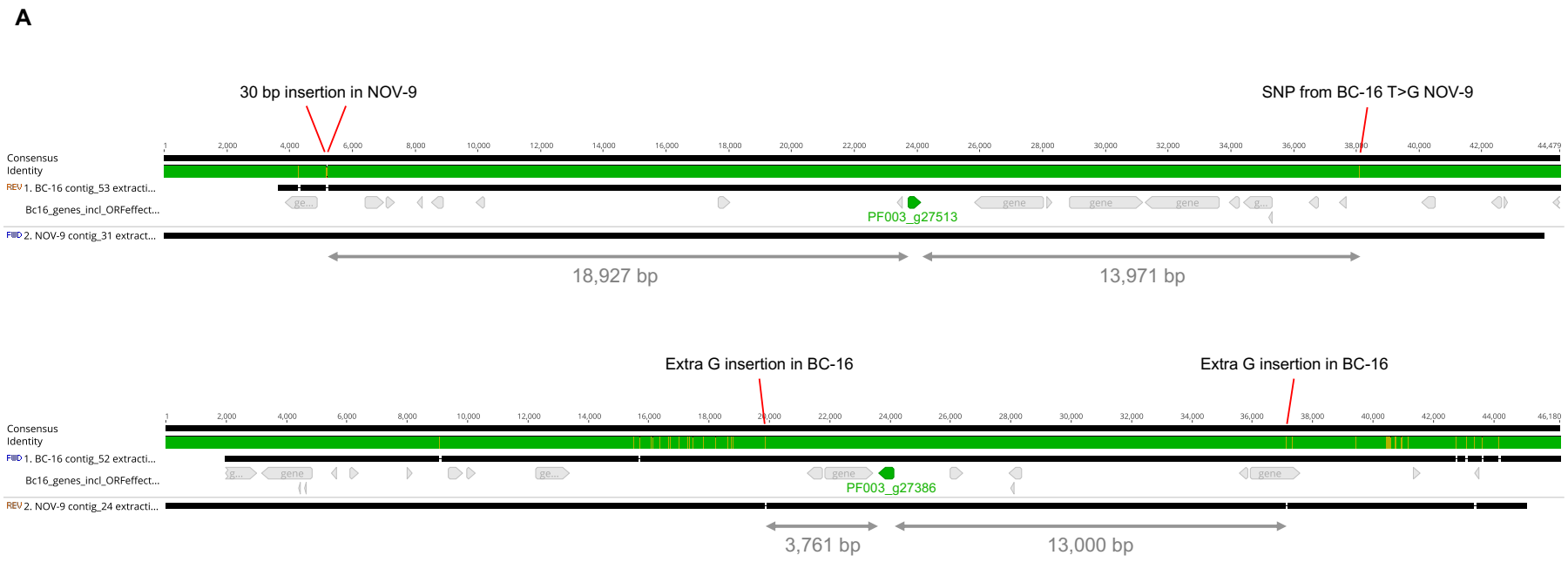

FIGURE 7 | Differential expression of putative *PfAvr2* and *PfAvr3* is not due to sequence variation in *Phytophthora fragariae* BC-16 (UK2) and NOV-9 (UK3) genomes. Regions surrounding candidate avirulence genes, *PfAvr2* and *PfAvr3*, from BC-16 and NOV-9 aligned with MAFFT in Geneious R10 (Katoh et al., 2002; Katoh and Standley, 2013). (**A**) Putative *PfAvr2*, showing a 30 bp insertion in the NOV-9 sequence upstream of PF003_g27513 and a T to G SNP in NOV-9 downstream of the gene of interest. (**B**) Putative *PfAvr3*, showing an extra G insertion in BC-16 upstream of PF003_g27386 (an orthologue of PF009_g26267) and an extra G insertion in BC-16 3,761 bp downstream.

TABLES

TABLE 1 | Summary of *Phytophthora fragariae* and *Phytophthora rubi* isolates used in this study.

Isolate Name	Species	Location	Date Isolated	Isolated by	Pathogenicity Race
A4	*Phytophthora fragariae*	Unknown	17/12/2001	Unknown	US4
BC-1	*Phytophthora fragariae*	Commercial Strawberry Field, Delta, BC, Canada	05/01/2007	N. L. Nickerson	CA1 (UK1)
BC-16	*Phytophthora fragariae*	Commercial Strawberry Field, Ladner, BC, Canada	05/01/2007	N. L. Nickerson	CA3 (UK2)
BC-23	*Phytophthora fragariae*	Commercial Strawberry Field, Aldergrove, BC, Canada	30/01/2012	N. L. Nickerson	CA5
NOV-5	*Phytophthora fragariae*	Commercial Strawberry Field, Nine Mile River, Hants County, NS, Canada	17/12/2001	N. L. Nickerson	CA1
NOV-9	*Phytophthora fragariae*	Commercial Strawberry Field, Billtown, Kings County, NS, Canada	05/01/2007	N. L. Nickerson	CA2 (UK3)
NOV-27	*Phytophthora fragariae*	Commercial Strawberry Field, Cambridge Station, Kings County, NS, Canada	19/12/2001	N. L. Nickerson	CA2
NOV-71	*Phytophthora fragariae*	Commercial Strawberry Field, Middle Clyde River, Shelburne County, NS, Canada	05/01/2007	N. L. Nickerson	CA2
NOV-77	*Phytophthora fragariae*	Commercial Strawberry Field, Nine Mile River, Hants County, NS, Canada	30/01/2012	N. L. Nickerson	CA5
ONT-3	*Phytophthora fragariae*	Commercial Strawberry Field, Fort Erie, ON, Canada	05/01/2007	N. L. Nickerson	CA4
SCRP245	*Phytophthora fragariae*	Kent, England, UK	1945	Unknown	Unknown
SCRP249	*Phytophthora rubi*	Germany	1985	Unknown	1
SCRP324	*Phytophthora rubi*	Scotland, UK	1991	Unknown	1
SCRP333	*Phytophthora rubi*	Scotland, UK	1985	Unknown	3

TABLE 2 | *Phytophthora fragariae* race structure detected by three differential strawberry (*Fragaria* × *ananassa*) accessions and categorisation into UK race scheme.

Cultivar[a]	Mock	*Phytophthora fragariae* Isolate[b]						
		BC-1	BC-16	NOV-9	A4	NOV-27	NOV-5	NOV-71
Allstar[1, 2, 3]	$0^{4/4}$	$0^{8/8}$	$0^{7/7}$	$0^{4/4}$	$0^{3/4}$	$0^{2/3}$	$0^{3/3}$	$0^{4/5}$
Cambridge Vigour[2, 3]	$0^{5/5}$	$+^{7/9}$	$0^{5/5}$	$0^{8/8}$	$0^{5/5}$	$0^{4/5}$	$+^{5/5}$	$0^{4/5}$
Hapil	$0^{12/12}$	$+^{10/10}$	$+^{10/10}$	$+^{10/10}$	$+^{4/5}$	$+^{5/5}$	$+^{3/5}$	$+^{5/5}$
Redgauntlet[2]	$0^{12/12}$	$+^{7/10}$	$0^{9/10}$	$+^{9/10}$	$0^{5/5}$	$+^{5/5}$	$+^{5/5}$	$+^{5/5}$
Deduced UK race	N/A	Race 1	Race 2	Race 3	Race 2	Race 3	Race 1	Race 3

[a] Known resistance genes in the *Fragaria* × *ananassa* cultivars.
[b] Number of replicates showing the recorded phenotype compared to the number of replicates tested; "+" representing a successful infection and "0" representing resistance.

TABLE 3 | Long read PacBio sequencing generated a highly contiguous *Phytophthora fragariae* BC-16 (UK2) reference genome. Assembly and annotation statistics compared to *Phytophthora sojae* P6497 (Tyler et al., 2006). Values in brackets include low confidence gene models from open reading frames.

	***Phytophthora fragariae* BC-16**	***Phytophthora sojae* P6497**
Assembly size (Mb)	90.97	82.60
Number of contigs	180	862
N50 (kb)	923.5	386.0
L50	33	61
Repeatmasked	38%	29%
Genes	37,049 (41,103)	26,584
RxLRs	486 (1,052)	350
CRNs	82 (85)	40
Apoplastic effectors	1,274 (4,757)	N/A

TABLE 4 | Comparable assembly statistics and gene predictions in resequenced isolates of *Phytophthora fragariae* and *Phytophthora rubi*.

	Phytophthora fragariae											*Phytophthora rubi*		
	A4	**BC-1**	**BC-16**	**BC-23**	**NOV-5**	**NOV-9**	**NOV-27**	**NOV-71**	**NOV-77**	**ONT-3**	**SCRP245**	**SCRP249**	**SCRP324**	**SCRP333**
Assembly Size (Mb)	79.08	79.10	90.97	78.26	78.99	79.43	79.75	78.37	78.80	79.06	77.84	77.79	77.91	77.82
Contig Number (≧ 500 bp)	13,446	11,556	180	13,191	13,531	11,801	12,489	12,212	13,321	13,265	13,231	14,023	13,946	13,679
N50 (kb)	18.2	21.8	923.5	18.2	17.9	21.5	19.4	20.2	18.9	18.8	18.2	16.6	16.9	16.9
L50	1,116	953	33	1,119	1,134	978	1,046	1,016	1,101	1,104	1,120	1,232	1,218	1,210
Repeatmasked	31%	31%	38%	31%	31%	31%	31%	31%	31%	31%	31%	31%	31%	30%
Genes[a]	30,180 (33,623)	30,375 (33,691)	37,049 (41,103)	29,960 (33,143)	30,248 (33,699)	29,986 (33,527)	30,600 (33,797)	29,708 (33,143)	30,099 (33,580)	30,180 (33,415)	30,202 (33,223)	31,458 (34,139)	30,235 (33,263)	32,623 (35,223)
Single-Copy BUSCO genes	274 (90%)	274 (90%)	266 (88%)	275 (91%)	273 (90%)	273 (90%)	273 (90%)	274 (90%)	272 (90%)	277 (91%)	273 (90%)	273 (90%)	274 (90%)	275 (91%)
Duplicated BUSCO genes	6 (2%)	6 (2%)	9 (3%)	5 (2%)	7 (2%)	6 (2%)	6 (2%)	6 (2%)	8 (2.5%)	7 (2%)	7 (2.5%)	8 (3%)	8 (3%)	7 (2%)
Fragmented BUSCO genes	6 (2%)	6 (2%)	5 (1.5%)	7 (2%)	6 (2%)	7 (2%)	7 (2%)	6 (2%)	6 (2%)	4 (1%)	7 (2.5%)	3 (1%)	3 (1%)	3 (1%)
Missing BUSCO genes	17 (6%)	17 (6%)	23 (7.5%)	16 (5%)	17 (6%)	17 (6%)	17 (6%)	17 (6%)	17 (5.5%)	15 (5%)	16 (5%)	19 (6%)	18 (6%)	18 (6%)

[a] Values in brackets include low confidence gene models from open reading frames.

TABLE 5 | Effector gene predictions in resequenced isolates of *Phytophthora fragariae* and *Phytophthora rubi*.

	Phytophthora fragariae											*Phytophthora rubi*		
	A4	**BC-1**	**BC-16**	**BC-23**	**NOV-5**	**NOV-9**	**NOV-27**	**NOV-71**	**NOV-77**	**ONT-3**	**SCRP245**	**SCRP249**	**SCRP324**	**SCRP333**
Secreted proteins[a]	3,637	3,601	4,217	3,611	3,626	3,637	3,690	3,633	3,620	3,658	3,581	3,697	3,683	3,832
RxLR HMM[b]	194	194	218	188	196	186	183	191	166	191	196	197	195	207
RxLR-EER Regex[c]	178	184	208	176	186	174	172	182	150	178	185	188	176	188
RxLR Regex	371	367	445	364	370	356	369	374	341	367	370	363	350	359
Final RxLR effectors[d]	410 (935)	405 (919)	486 (1,052)	402 (928)	408 (918)	397 (951)	405 (899)	412 (931)	378 (934)	403 (898)	407 (882)	407 (882)	395 (861)	410 (826)
CRN LFLAK HMM[c]	85	83	114	86	84	82	87	90	86	90	90	156	93	154
CRN DWL HMM[c]	95	87	121	96	91	96	93	101	83	90	87	139	102	142
Final CRNs[d,e]	55 (68)	53 (59)	82 (87)	55 (62)	53 (67)	50 (61)	57 (63)	59 (71)	62 (75)	61 (74)	60 (68)	128 (132)	71 (85)	128 (134)
Apoplastic effectors[d,f]	991 (3,896)	1,002 (3,798)	1,274 (4,757)	980 (3,630)	986 (3,913)	1,007 (3,983)	1,011 (3,708)	1,007 (3,911)	1,010 (3,922)	982 (3,709)	984 (3,522)	1,017 (3,266)	1,059 (3,607)	1,090 (3,268)

[a] SignalP: Nielsen et al., 1997; Bendtsen et al., 2004; Petersen et al., 2011 and Phobius: Käll et al., 2007.
[b] Whisson et al., 2007.
[c] Armitage et al., 2018.
[d] Values in brackets include low confidence gene models from open reading frames.
[e] Both LFLAK and DWL HMM models present (Armitage et al., 2018).
[f] ApoplastP: Sperscneider et al., 2018.

TABLE 6 | Conserved putative core *Phytophthora fragariae* RxLR effector candidates important for pathogenicity on strawberry (*Fragaria* × *ananassa*) from isolates BC-1, BC-16 and NOV-9. Conserved RxLR candidates in the 50 highest expressed genes *in planta* with a log fold change (LFC) of ≥3, based on comparison to respective mycelium. The BC-16 24 hour post inoculation (hpi) timepoint was used for BC-16.

Orthogroup	BC-16 gene ID	Fragments Per Kilobase of transcript per Million mapped reads (FPKM)								Avr homology
		BC-1 (UK1)		BC-16 (UK2)				NOV-9 (UK3)		
		Mycelium	48 hpi	Mycelium	24 hpi	48 hpi	96 hpi	Mycelium	72 hpi	
OG0010423	PF003_g35418	94	5,354	192	6,578	4,986	2,961	12	3,868	
OG0018019	PF003_g6480	241	3,544	235	2,113	1,977	1,717	231	2,501	
OG0011458	PF003_g16448	4	2,899	4	4,656	2,108	1,090	7	1,699	*P. sojae Avr1b*[a]
OG0021012	PF003_g16234	36	1,345	31	1,181	827	674	23	737	

[a] Top hit from GenBank tblastn search is AF449623, *Phytophthora sojae Avr1b* (Shan et al., 2004).

919 **SUPPLEMENTARY MATERIAL**

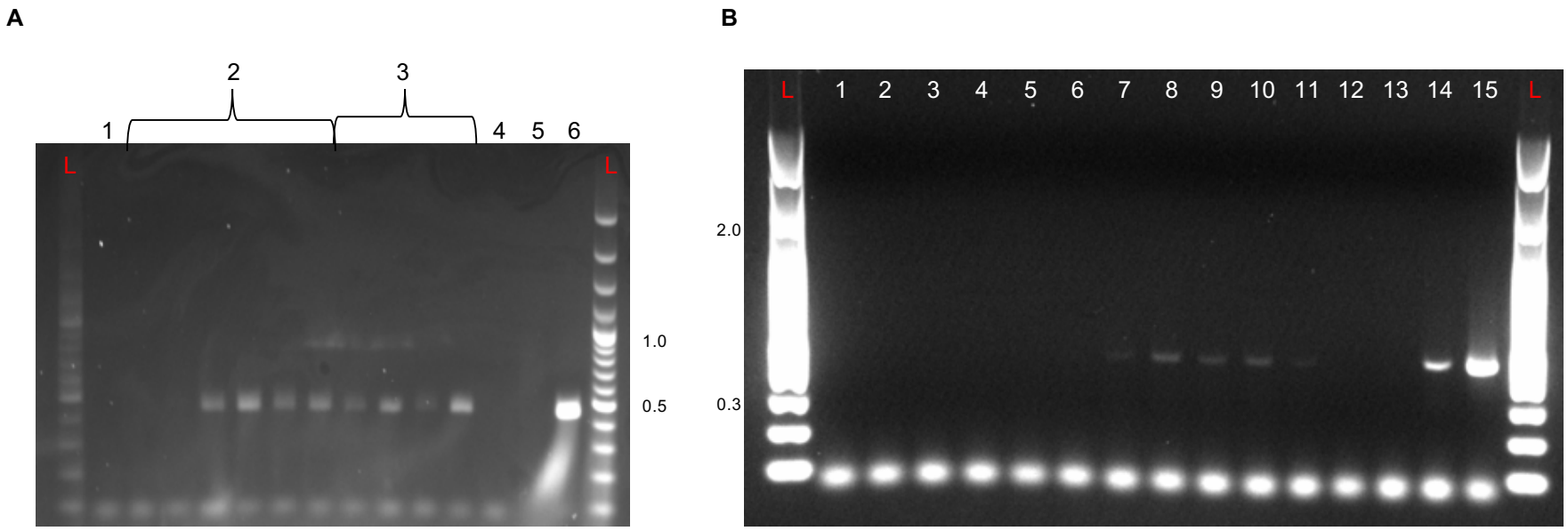

920

921 **SUPPLEMENTARY FIGURE S1 | Agarose gel electrophoresis of RT-PCR reactions on representative samples from inoculation**
922 **time course experiments on the 'Hapil' cultivar of *Fragaria* × *ananassa*. A:** Gel of samples from an inoculation time course experiment
923 with the BC-16 isolate of *Phytophthora fragariae*. **L:** 100 bp Plus Ladder (ThermoFisher Scientific, Waltham, MA, USA) sizes listed in
924 kb. **1:** Mock inoculated *Fragaria* × *ananassa* cultivar 'Hapil' plant. **2:** Time course of inoculated plants with stream water used as the
925 flooding solution. Time points from left to right: 24 hpi, 48 hpi, 96 hpi, 144 hpi, 192 hpi and 240 hpi. **3:** Time course of inoculated plants
926 with Petri's solution used as the flooding solution. Time points from left to right: 24 hpi, 48 hpi, 96 hpi and 144 hpi. **4:** dH2O control. **5:**
927 'Flamenco' gDNA control. **6:** BC-16 gDNA control. **B**: Gel of samples from an inoculation time course experiment with the BC-1 and
928 NOV-9 isolates of *P. fragariae*. **L**: 100 bp plus ladder from New England Biolabs, sizes listed in kb. PCR templates: **1**: Uninoculated plant
929 cDNA. **2**: NOV-9 12 hours post inoculation (hpi) cDNA. **3**: BC-1 12 hpi cDNA. **4**: NOV- 9 24 hpi cDNA. **5**: BC-1 24 hpi cDNA. **6**: NOV-
930 9 48 hpi cDNA. **7**: BC-1 48 hpi cDNA. **8**: NOV-9 72 hpi cDNA. **9**: BC-1 72 hpi cDNA. **10**: NOV-9 96 hpi cDNA. **11**: BC-1 96 hpi cDNA.
931 **12**: dH2O. **13**: gDNA from a *F.* × *ananassa* cultivar 'Hapil' plant. **14**: gDNA from BC-16 mycelium. **15**: cDNA from BC-16 mycelium.

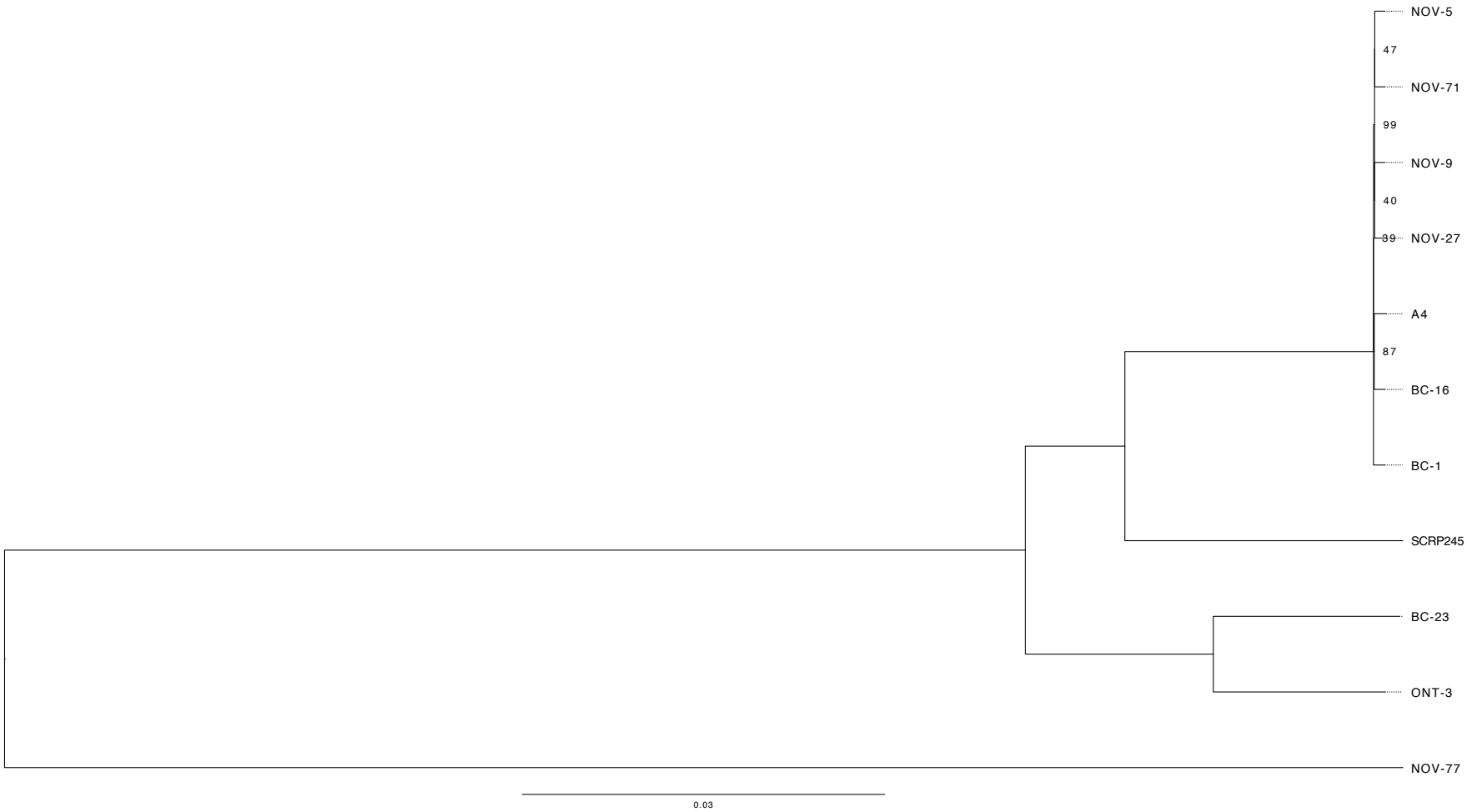

SUPPLEMENTARY FIGURE S2 | *Phytophthora fragariae* isolates separate into distinct clades. Neighbour joining tree based on high quality, biallelic SNP sites, node labels represent the number of bootstrap replicates supporting the node; only values less than 100 are shown.

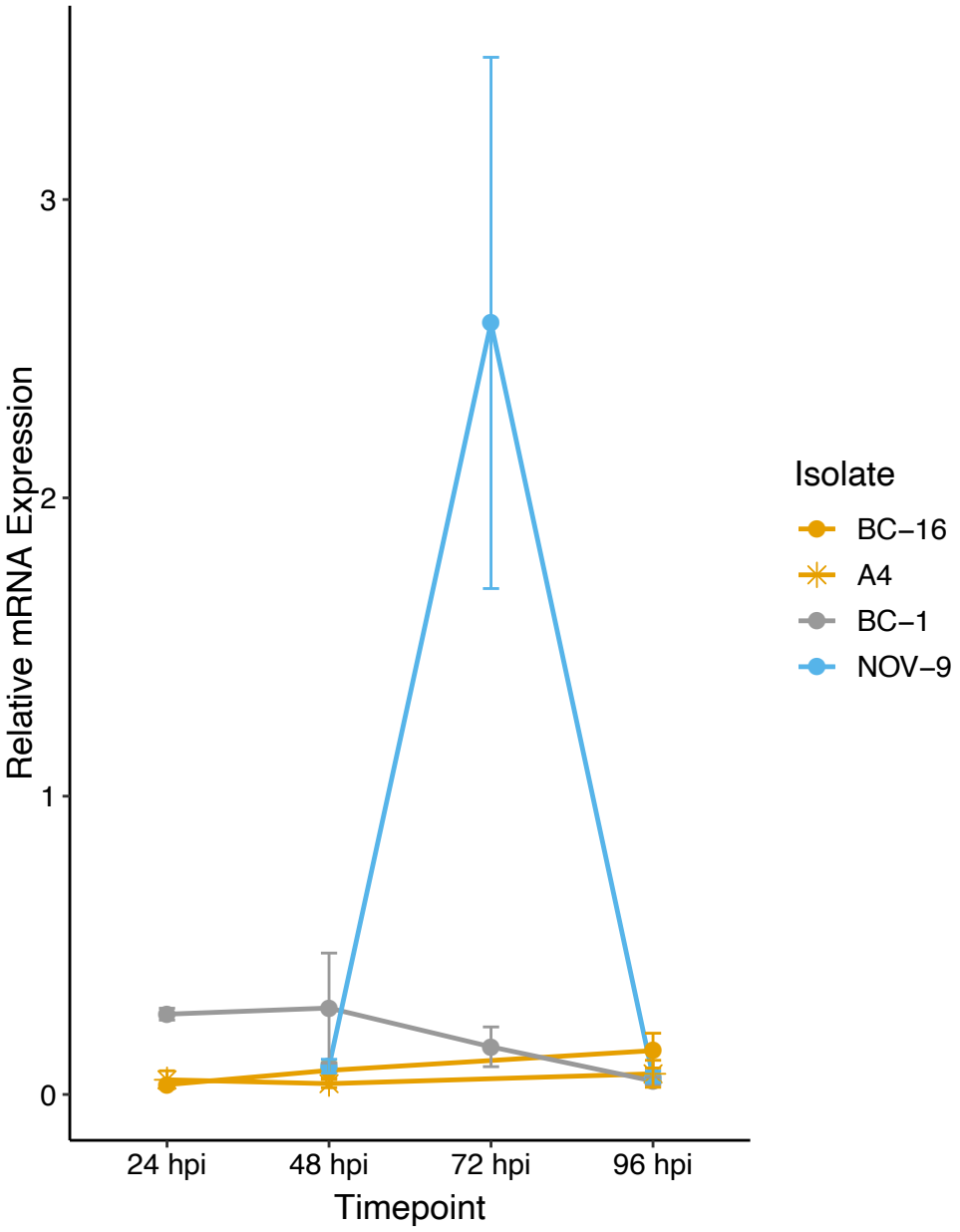

936

937 **SUPPLEMENTARY FIGURE S3 | *PfAvr3* candidate PF009_g26276 is differentially expressed**
938 **in *Phytophthora fragariae* UK-1-2-3 isolates.** Quantitative reverse transcription PCR of a candidate
939 for the avirulence gene possessed by NOV-9, but not BC-1, BC-16 and A4 (PF009_g26276.t1). Plots
940 created by the ggplot2 R package (Wickham, 2016) in R version 3.4.3 (R core team, 2017).

SUPPLEMENTARY TABLES

SUPPLEMENTARY TABLE S1 | Primers used in this study. Primers supplied by IDT (Leuven, Belgium).

Primer Name	Target	Gene Name	BC-16 Gene ID	Primer Sequence	Length (bp)	Reference
Pf_Btub_F Pf_Btub_R	RT-PCR	β-tubulin	PF003_g4288.t1	5'-GGATAACGAGGCCCTGTACG-3' 5'-TGTTGTTGGGGATCCACTCG-3'	440	This Study
WS41_163F WS41_318R	Housekeeping	WS41	PF003_g28439.t1	5'-ATCGTGCTGTACCTGGGC-3' 5'-GATCTCGCTGGGCTTGAAGG-3'	156	This Study
Btub_44F Btub_152R	Housekeeping	β-tubulin	PF003_g4288.t1	5'-CCGCGCCCGTACAGCAAC-3' 5'-TCGGAGATGACTTCCCAGAACTTG-3'	109	This Study
cAvr2_65F cAvr2_244R	Candidate Race 2 *Avr* Gene	Candidate *PfAvr2*	PF003_g27513.t1	5'-TGTCAAAGGCCGATCAGAGC-3' 5'-CGAACAAACTATCCACACCAGC-3'	180	This Study
cAvr3_F cAvr3_R	Candidate Race 3 *Avr* Gene	Candidate *PfAvr3*	PF003_g27386.t1	5’-ACAAGATGGACCCGAACCTCAT-3’ 5’-CAACCTCCTGACAGCTCCTTCAAC-3’	209	This Study
U16SRT-F U16SRT-R	Inter-plate calibrator	16S	N/A	5'-ACTCCTACGGGAGGCAGCAGT-3' 5'-TATTACCGCGGCTGCTGGC-3'	180	Clifford et al., 2012

SUPPLEMENTARY TABLE S2 | Details of expression of genes surrounding putative *PfAvr2* (PF003_g27513).

			Fragments Per Kilobase of transcript per Million mapped reads (FPKM)							
	Orthogroup	**BC-16 gene ID**	**BC-1**		**BC-16**				**NOV-9**	
			Mycelium	**48 hpi**	**Mycelium**	**24 hpi**	**48 hpi**	**96 hpi**	**Mycelium**	**72 hpi**
	OG0003811	PF003_g27515	0	0	0	0	0	0	0	0
	OG0000375	PF003_g27514	476	546	11	248	260	206	58	80
Putative *PfAvr2*	**OG0026610**	**PF003_g27513**	**0**	**0**	**1**	**9,392**	**6,263**	**3,075**	**0**	**33**
	OG0000960	PF003_g27512	3	1	0	0	0	1	2	2
	OG0036362	PF003_g27511	0	0	0	0	0	0	--	--

SUPPLEMENTARY TABLE S3 | Details of expression of genes surrounding putative *PfAvr3* (PF003_g27386/PF009_g26276).

			Fragments Per Kilobase of transcript per Million mapped reads (FPKM)							
	Orthogroup	**BC-16 gene ID**	**BC-1**		**BC-16**				**NOV-9**	
			Mycelium	**48 hpi**	**Mycelium**	**24 hpi**	**48 hpi**	**96 hpi**	**Mycelium**	**72 hpi**
	OG0002229	PF003_g27388	0	0	0	0	0	0	0	0
	OG0003130	PF003_g27387	0	0	0	0	0	0	0	0
Putative *PfAvr3*	**OG0018589**	**PF003_g27386**	**17**	**6**	**10**	**12**	**4**	**4**	**16**	**199**
	OG0018588	PF003_g27385	38	33	26	36	64	78	29	61
	OG0018587	PF003_g27384	0	0	0	0	0	0	1	1

941 **SUPPORTING TABLES**

942 **SUPPORTING CANDIDATE TABLE | Gene names of all genes identified as putative candidate**
943 **avirulence genes for *Phytophthora fragariae* UK1, UK2 and UK3.**

944 Gene names are listed with respect to the isolate for which they are described as candidate avirulence
945 genes.

946

947 **SUPPORTING ANNOTATION TABLE | Details of all predicted genes in *Phytophthora***
948 ***fragariae* UK2 isolate BC-16.**